Geological Society of America
Memoir 151

Development of monoclines: Part II. Theoretical analysis of monoclines

ZE'EV RECHES
Weizmann Institute
Rehovot, Israel

ARVID M. JOHNSON
Department of Geology
University of Cincinnati
Cincinnati, Ohio 45221

ABSTRACT

Monoclinal flexures, which are isolated asymmetric flexures, range in scale from a few millimetres in kink bands to hundreds of metres in monoclines on the Colorado Plateau. A general model of monoclinal flexuring of multilayers is proposed here; the multilayers include layers with various rheologies, densities, thicknesses, and strengths of contacts between layers. The multilayers are subjected to displacements at their base, stresses at their edges, and a free surface at their tops. We study in detail three modes of this general model, assuming linear, incompressible elastic or viscous multilayers: *Drape folding,* in which a monoclinal flexure develops over a vertical fault; *buckling,* in which an initial monoclinal flexure is amplified by layer-parallel compression; and *kinking,* in which monoclinal kink bands develop unstably by compression inclined to the layering. Selected solutions are presented for the first two modes, and previous research is summarized for the kinking mode.

According to analyses of the three special cases of the general model, the profile of the monoclinal flexure, the displacement field, and the strain distribution within the flexure are useful criteria for distinguishing among the three modes of monoclinal flexuring. The Palisades monocline, described in detail in Part I (this volume), is interpreted to be a result of a combination of drape folding over a fault in Precambrian basement rocks and buckling, which together appear to account for most of the field observations. The Yampa monocline in Dinosaur National Park changes form along its length, but each form can be compared with characteristics of a combination of modes, including faulting at depth and layer-parallel compression. In some places it closely resembles a large kink band.

INTRODUCTION

Monoclinal flexures, which are isolated asymmetric flexures, range widely in scale and in tectonic setting. The smallest monoclinal flexures are kink bands, typically a few millimetres to a few hundred metres wide (Fig. 1A), which apparently form in response to a combination of layer-parallel shortening and shear in certain foliated materials; they are a buckling and shearing phenomenon (Reches and Johnson, 1976). Monoclinal flexures have developed at edges of several laccolithic intrusions also (Johnson and Pollard, 1971; Johnson and Ellen, 1974). Figure 1B shows a monoclinal flexure, with a width of about 100 m, at one edge of a laccolithic intrusion in the Henry Mountains of Utah. This flexure presumably formed in response to uplift of the sedimentary rocks by pressure in the magma of the intrusion. The largest of the monoclinal flexures are *monoclines* themselves, which occur in the Rocky Mountains, on the margin of the Arabo-Nubian massif, on the Colorado Plateau, and in other areas of the world. For example, Figure 1C shows a structural cross section of the East Kaibab monocline in Palisades Creek, Grand Canyon National Park (Reches, this volume). Although this paper is primarily concerned with mechanical analysis of large monoclines such as the East Kaibab, a complete mechanical analysis of monoclinal flexures must be capable of explaining other monoclinal flexures as well.

Monoclines normally are explained as drape folds, so that the flexure in the sedimentary sequence is assumed to have been the passive response of the sequence to displacement along a fault at its base (Prucha and others, 1965; Stearns, 1971). A necessary conclusion from this concept of drape folding is that the layers should be extended in the anticlinal part of the monocline if the dip and displacement of the fault below are vertical (Sanford, 1959). However, several investigators have noted evidence for significant shortening of layers within monoclines (Walcott, 1890; Baker, 1935; Kelley, 1955; Reches, this volume). Kelley (1955) examined most of the monoclines on the Colorado Plateau and reported widespread evidence of layer-parallel shortening. Detailed study of the East Kaibab monocline in Palisades Creek (Reches, this volume), indicates abundant evidence for layer-parallel shortening within and near the monocline. It is well known that layered sequences of rock subjected to layer-parallel shortening tend to buckle, so it is possible that many monoclines have developed partly by buckling, not merely by passive drape folding in response to faulting below.

The first part of this series (Reches, this volume) outlined an approach to the study of monoclines and presented the results of detailed field study. Theoretical analysis was avoided in the first part, and discussion was limited to interpretation of observations. Now we shall primarily discuss theories of monoclinal flexuring.

The purpose of this paper is to explore a relatively general theoretical model of monocline formation in multilayers, including effects of properties of contacts between layers, of dimensional and rheological properties of the layers, and of layer-parallel shortening and faulting displacement at the base of the multilayer. First, we shall define and describe the general model and define three special models that we have chosen to analyze. Then, we shall present and discuss the most important results of theoretical analyses of these three models; details of the theoretical analyses are presented in appendixes. And finally, we shall discuss the limitations of the theory and apply relevant results to several field and experimental examples.

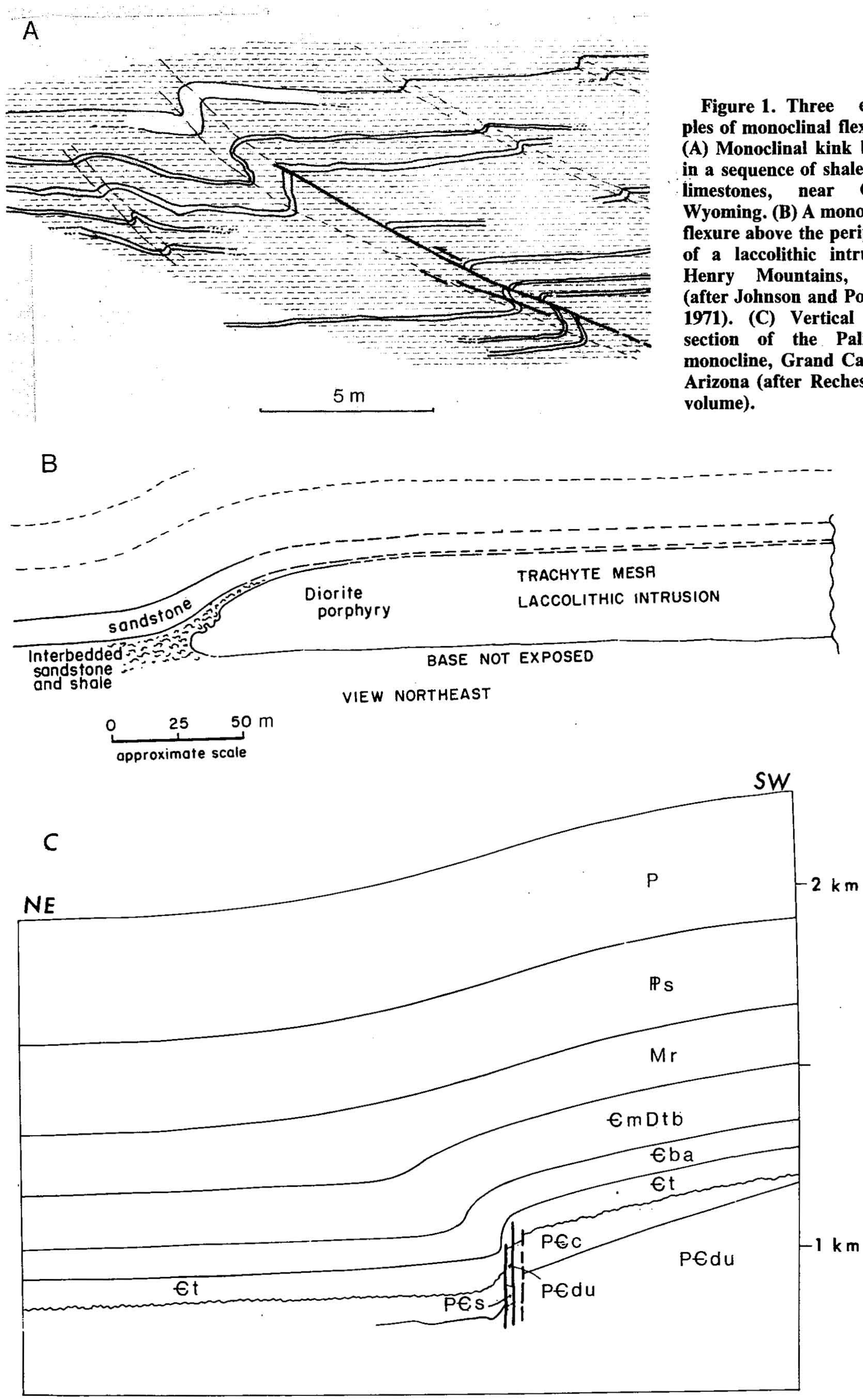

Figure 1. Three examples of monoclinal flexures. (A) Monoclinal kink bands in a sequence of shales and limestones, near Cody, Wyoming. (B) A monoclinal flexure above the periphery of a laccolithic intrusion, Henry Mountains, Utah (after Johnson and Pollard, 1971). (C) Vertical cross section of the Palisades monocline, Grand Canyon, Arizona (after Reches, this volume).

GENERAL MODEL OF MONOCLINAL FLEXURING

The occurrence of monoclinal flexures in a wide variety of rock types and tectonic settings and over a wide range of scales (Fig. 1) suggests that there are several mechanisms that can be responsible for the formation of monoclines. We would suggest a general model of monoclinal flexuring that incorporates all known mechanisms as well as a variety of material properties and boundary conditions (Fig. 2). The general model includes a multilayer with a free surface above and with a substratum below, subjected to various boundary conditions. The upper surface and the contact between the multilayer and the substratum might be planar or irregular. Displacement (U and V, Fig. 2) boundary conditions may be specified at the interface between the substratum and the multilayer. Also, the multilayer may be subjected to layer-parallel compression or extension (S_{xx}, Fig. 2). Further, the multilayer itself may have a wide range of dimensional and rheological properties. The layers might be elastic, viscous, or power-law materials. The contacts between layers might be frictionless, allowing free slip, or bonded, allowing no slip, or they might be described in terms of a yield strength, so that slippage between layers is possible if the shear stress equals some critical value. Finally, the multilayer might consist of interbedded stiff and soft layers with various thicknesses, or might even consist of a single layer. This is our general model of monocline formation. The theoretical problem is to determine conditions under which ideal monoclinal flexures might develop in such a model.

The general model of monocline formation is much too complicated to analyze completely; the number of combinations of variables is overwhelming. However, based on field observation, experimentation, and preliminary theoretical analysis, we can eliminate many combinations of variables. Thus, we know that layer-parallel extension tends to retard buckling, so we can specify that the layer-parallel stress, S_{xx}, is either zero or compressive. Similarly, we know that irregular interfaces of layers tend to induce irregular fold patterns, so we can simplify the analysis by assuming that the interfaces originally are planar or have certain simple forms, without the risk of losing fundamental insights into processes of monocline formation. The remaining variables in our general model are numerous, and in order to restrict them somewhat, we shall make rather arbitrary choices. Thus, we shall consider

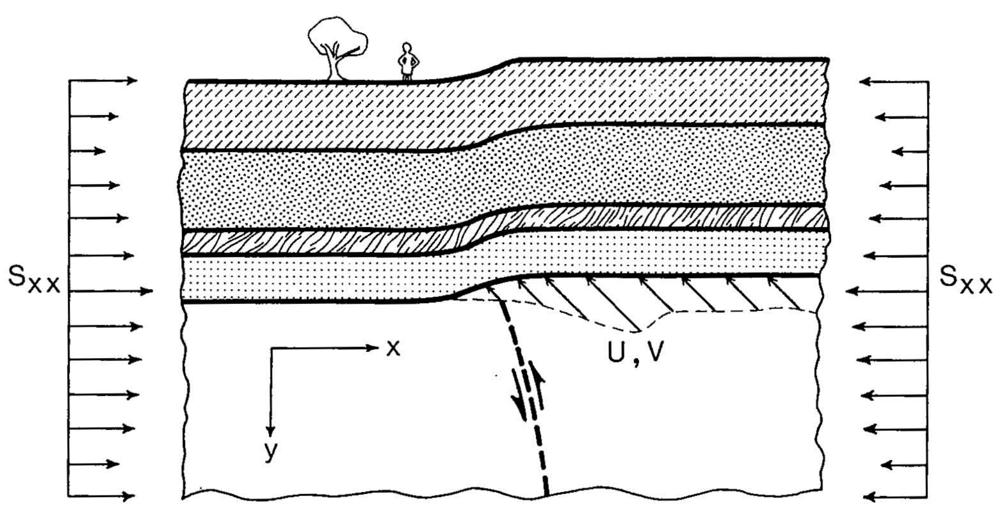

Figure 2. Schematic presentation of the general model of monoclinal flexuring. U and V are displacements of the base of the multilayer and S_{xx} is the horizontal stress. The layers may have various densities, rheologies, and thicknesses.

TABLE 1. SUMMARY OF ESSENTIAL FEATURES OF THE GENERAL MODEL OF MONOCLINES AND OF THE THREE SPECIAL CASES

General model		
Multilayer comprised of layers with elastic or viscous and linear or nonlinear rheologic properties. Finite contact strength. Finite strain. Includes effects of gravity. Displacement and stress boundary conditions.		
Special models		
Drape folding	Buckling	Kinking
Linear elastic or viscous layers. Infinite or zero contact strength. Vertical displacement at base. Infinitesimal plane strain.	Linear elastic or viscous layers. Infinite or zero contact strength. Layer-parallel shortening. Infinitesimal plane strain.	Elastic, or elastic-plastic layers. Finite contact strength. Layer-parallel shortening and shear. Finite plane strain. Large slopes.

multilayers with bonded or frictionless contacts as well as multilayers which have finite contact strengths. These three choices cover a wide range of properties of contacts. Finally, we shall assume that the multilayer is comprised of linear elastic or viscous layers. We shall not specifically study effects of compressibility, of nonlinear elastic, or of power-law behaviors here, but we know from other analyses of folding (Fletcher, 1974; Johnson, 1977, chap. 10) that general conclusions derived from one of these behaviors are valid for all the materials. Thus, we know that first-order analysis of nonlinear materials would not contribute fundamentally to our understanding of conditions of monoclinal flexuring (Johnson, 1977, chap. 10).

These considerations allow us to restrict our analysis to three special cases of our general model of monocline formation, and we have chosen to analyze these three models in some detail here (Table 1). We shall call them "drape folding," "buckling," and "kinking."

Drape Folding

The idea that monoclines are a response of a sedimentary sequence to faulting at its base was suggested by early investigators of monoclines, including Powell (1873) and Dutton (1882). This idea of drape folding of a multilayer is so simple and sound that it has been adopted by many geologists. Several theoretical analyses of drape folding have been published (Sanford, 1959; Howard, 1966; Min, 1974; Zanemonets and others, 1976).

According to the model of drape folding, the multilayer is deformed by displacement along its base (displacements U and V, Fig. 2). The multilayer might respond passively to these boundary displacements, where we use the term "passive" to imply that no mechanical instabilities are induced in multilayer, and in general the multilayer would deform much as a single layer, as analyzed by Sanford (1959). Several investigators have suggested that drape folding is a result of the contrast in mechanical properties between the faulted and stiff basement below and the layered and soft sedimentary cover above (Prucha and others, 1965; Stearns, 1971). However, our field observations (Fig. 1C), as well as our preliminary theoretical analysis of drape folding, indicate that the mechanism of deformation of the sedimentary cover is virtually independent of the source of displacement at the base. For example, a vertical fault in sedimentary rocks (Fig. 1C), a laccolithic intrusion of viscous magma (Fig. 1B), and a flexure of the basement surface would cause similar deformation in the sedimentary rocks above. Therefore, the development of monoclinal flexures by drape folding is not restricted to regions in which soft sediments are underlain by stiff basement.

It has been suggested that monoclinal flexures can form over both normal and reverse faults (Walcott, 1890; Baker, 1935; Stearns, 1971). However, analysis of drape folding should be restricted to boundary displacements normal (V, Fig. 2) to layering, such as those of a vertical fault, because displacements parallel (U, Fig. 2) to layering will cause the multilayer to shorten or lengthen. Any analysis that includes layer-parallel boundary displacements and ignores the layer-parallel deformation is incomplete. For example, layer-parallel shortening can lead to buckling.

We shall study the deformation of a horizontal multilayer due to displacement along a vertical fault at its base (Fig. 3B). The multilayer would accommodate the displacement of the base by draping over the fault to form a continuous flexure, by yielding, by faulting into several blocks, or by a combination of draping and faulting. We will analyze the draping mode only, because the faulting mode is beyond the limits of current theory.

Buckling

Walcott (1890) studied the East Kaibab monocline in the Grand Canyon area and suggested, apparently for the first time, that buckling processes are important in the development of monoclines. Other investigators (Baker, 1935; Kelley, 1955) recognized evidence of layer-parallel shortening within many monoclines, and they suggested that the monoclines are merely drape folds over reverse faults. They ignored possible effects of layer-parallel shortening on growth of the monocline itself; they imagined that layer-parallel shortening was required merely to account for compressional features such as small folds and reverse faults within the monoclines.

However, according to the general model of monoclinal flexuring, a possible

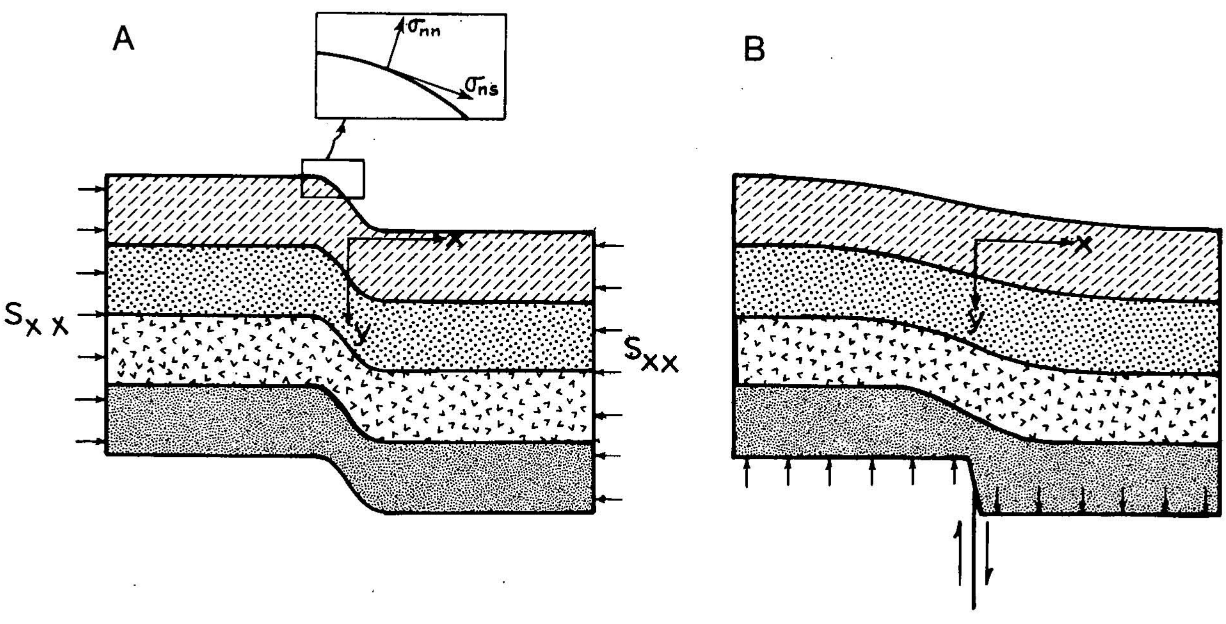

Figure 3. Boundary conditions of the buckling mode and the drape folding made of monoclinal flexuring. (A) The buckling is a result of shear, σ_{ns}, on inclined surfaces. (B) The drape folding is a result of displacement at base of flat multilayer.

way to generate a monocline is by buckling of the multilayer into an asymmetric fold. Folding theory indicates that a multilayer subjected to layer-parallel shortening tends to deflect into a train of folds, and that the amplification and shape of the folds depend on the properties of the multilayer (Ramberg, 1970; Johnson, 1970, 1977) and on the form of the initial deflection (Biot and others, 1961; Fletcher and Sherwin, 1978). On the other hand, it has been shown both experimentally and theoretically that asymmetric folds cannot initiate in a flat multilayer subjected to layer-parallel shortening and shear (Treagus, 1973; Reches and Johnson, 1976); rather, series of symmetric folds develop in such multilayers. Monoclinal flexures characteristically are isolated, asymmetric flexures and therefore cannot be simply related to repetitive, symmetric folds in a multilayer.

Even though a monoclinal flexure cannot develop spontaneously in a multilayer with initially flat contacts, it can develop in a multilayer with a low-amplitude, monoclinal initial deflection. A possible result of layer-parallel shortening of such a multilayer is amplification of the initial deflection into a large monoclinal flexure. The fundamental elements of this process of monocline formation can be elucidated by means of experimental and theoretical analyses of folding of a single stiff layer in a soft medium. Figure 4 shows results of three experiments with rubber layers of different thicknesses and properties embedded in thick gelatin media. All three rubber layers had the same initial monoclinal deflection (Fig. 4A1, B1, C1). Each rubber layer has a dominant wavelength defined approximately by the relation

$$W_d = 2\pi T \,[G_1/(6G_2)]^{1/3}, \tag{1}$$

where T is thickness and G_1 is shear modulus of the rubber layer and G_2 is shear modulus of the medium. The dominant wavelengths are shown in Figure 4A4, B4, C4; each corresponds with the wavelength that grows most rapidly with an increase in axial shortening.

In all three experiments the layer and gelatin were subjected to layer-parallel compression and layer-normal extension. In experiment A (Fig. 4A), the monocline grew in amplitude, and adjacent anticlines and synclines developed (Fig. 4A2). In experiment C (Fig. 4C), the monocline did not grow perceptibly; instead, many small folds developed along the rubber layer (Fig. 4C3).

Examination of the dominant wavelengths shown in Figure 4A4, B4, and C4 provides some insight into the differences among the three experiments. The dominant wavelength of the thick rubber layer in experiment A (Fig. 4A) is on the order of the width of the initial monoclinal deflection (Fig. 4A1), whereas the dominant wavelength of the thin rubber layer in experiment C (Fig. 4C4) is significantly shorter than the width of the initial monoclinal deflection (Fig. 4C). One may conclude that each rubber layer buckled according to its dominant wavelength, even though the initial deflections were the same. One can express this conclusion in a different form. The initial monoclinal shape can be described as the sum of an infinite number of sinusoidal waves (in the form of a Fourier series, equation 22a, App. 2). The dominant wavelength of the shortened rubber layer selectively amplifies more than the others (Johnson, 1970, p. 141). Accordingly, if the dominant wavelength of the layer is on the order of the width of the initial deflection (as in experiment A), the monocline will be strongly amplified, whereas if the dominant wavelength of the layer is significantly shorter than the initial deflection (as in experiment C), the monoclinal flexure will not be amplified significantly. If the dominant wavelength of the layer is much larger than the width of the initial deflection, the monoclinal flexure again will not be amplified significantly.

The same general conclusion applies to growth of initial deflections in multilayers, but the results are slightly more complex for several reasons. For example, a multilayer can have more than one dominant wavelength (Ramberg and Strömgård, 1971; Johnson and Page, 1976), so that folds with a range of wavelengths may amplify significantly. In our analysis we will investigate conditions that favor

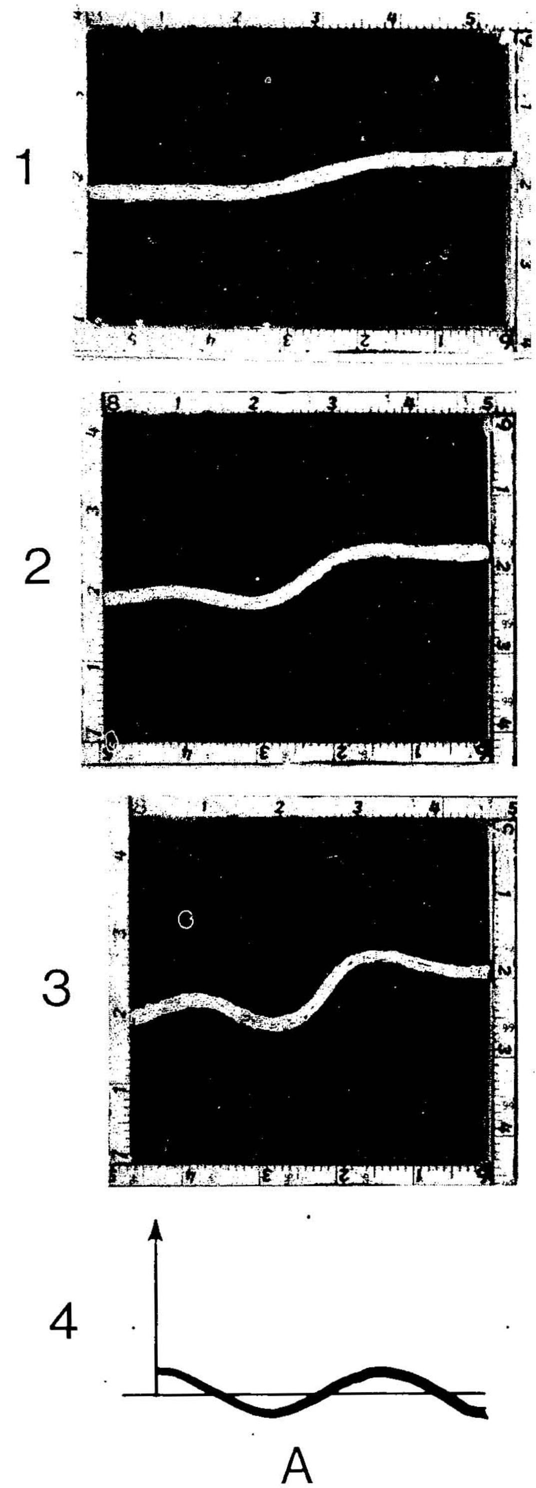

Figure 4. (facing pages). Three experiments of monoclinal flexuring of a rubber layer embedded in thick, soft gelatin. Plane strain, constant volume deformation was applied. The layers and the medium were both shortened horizontally. The initial monoclinal flexure is identical but the thickness of the rubber is different in the three experiments. Each unit on the frame of the folding machine is 3 cm. (1) The initial monoclinal flexure. The initial form was made by cutting the plate of gelatin to the desired curve. (2) The monoclinal flexure after small shortening. (3) The final monoclinal flexure. (4) The dominant wavelength for each experiment, calculated through equation (1).

amplification of initial monoclinal flexures in multilayers. We shall assume that small displacement along a vertical fault is amplified as a result of horizontal shortening. However, the initial deflection need not be restricted to a vertical fault; it could be the result of a local disturbance in the inclination of layers, such as a normal or reverse fault, or it could be the edge of an igneous intrusion

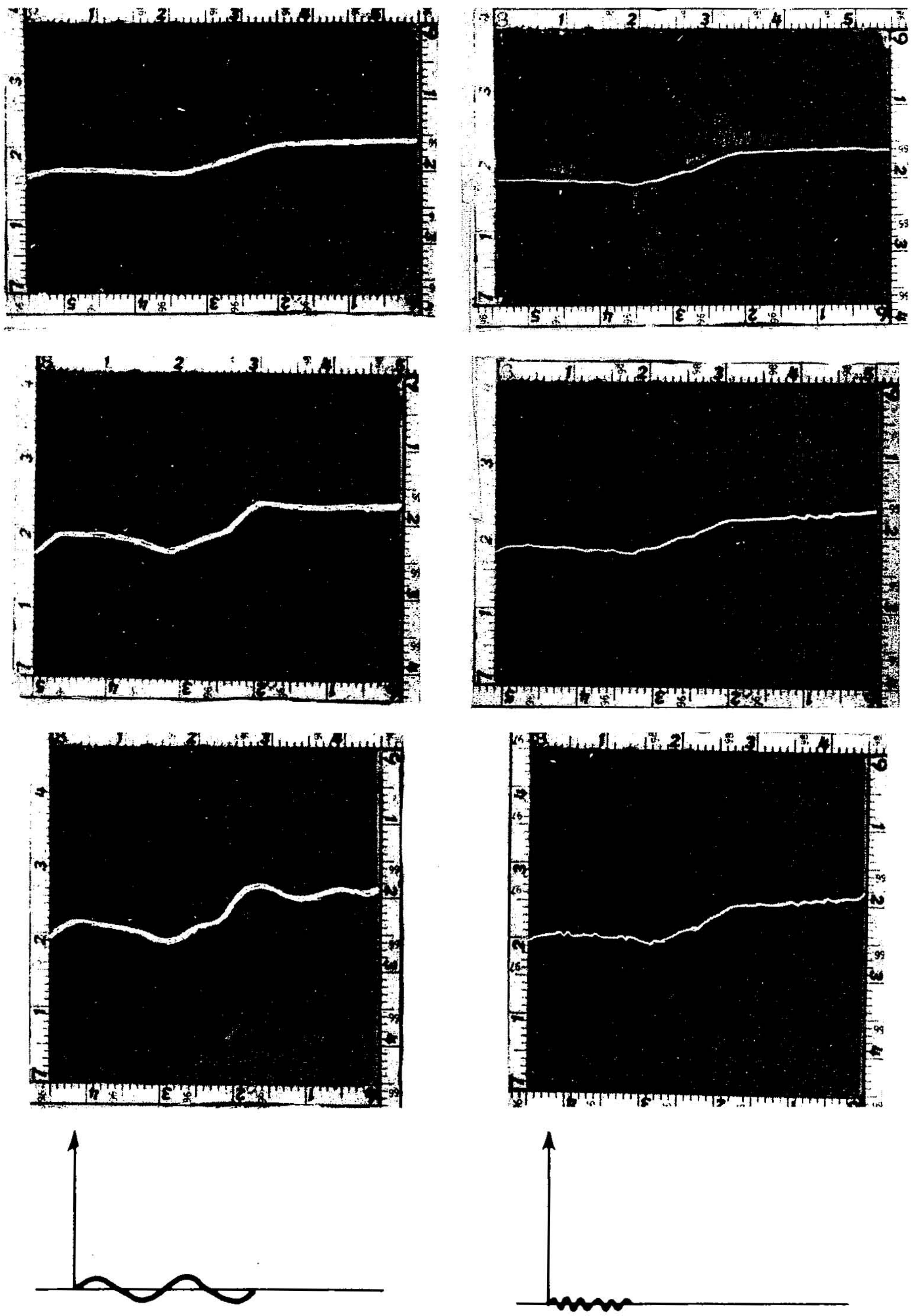

B C

or an unconformity in the sedimentary rock sequence. Thus, according to the concept of monoclinal flexuring by buckling, the initial deflection serves primarily as a localizer or trigger for the monoclinal flexure rather than as the cause of monoclinal flexure as in the concept of drape folding.

Kinking

The third special case of the general model of monoclinal flexuring which we shall analyze is that of kinking, a process that depends upon contact strength between layers being overcome locally to produce a local flexure or kink band. We have analyzed conjugate and monoclinal kinking in some detail elsewhere (Honea and Johnson, 1976; Reches and Johnson, 1976), so we shall restrict the discussion here to general conclusions. Kink bands are characterized by relatively straight limbs and tight hinge zones (Fig. 1A) and resemble some monoclines geometrically. According to our analyses of kink folding, the essential processes are buckling and yielding instabilities. The kinking mode is more nearly akin to the buckling mode of monocline formation discussed above than to the drape folding mode, because it requires that the direction of maximum compression be subparallel to layering.

Several examples of monoclinal kink bands in various types of multilayers are shown elsewhere (Johnson, 1970, p. 319; Ramberg and Johnson, 1976, Figs. 5, 11; Reches and Johnson, 1976, Figs. 2, 3, 4, 7). In all cases the multilayers were subjected to a combination of layer-parallel shortening and shear. For example, Figure 5A shows monoclinal kink bands in thin rubber strips, the contacts between which were unlubricated, so that the contact strength was frictional. The kink band developed as the layer-parallel shear and shortening were increased. Conjugate kink bands, in contrast, developed where multilayers were subjected to layer-parallel shortening, without shear (Honea and Johnson, 1976, Figs. 2, 3, 4).

A series of experiments that are particularly relevant to the general model of monocline formation was conducted with the same type of apparatus used to subject multilayers to simultaneous layer-parallel shear and shortening but, in addition, one segment of one side of the apparatus could be faulted by retracting the segment (Fig. 5B). Each multilayer was first subjected to layer-parallel shortening and shear, and then to faulting. In one experiment the shear induced by faulting was of the same sense as the shear induced by the loading frame (Fig. 5B). A left-lateral monoclinal kink band developed over the fault. Subsequently, another parallel monoclinal kink band developed nearby. In another experiment the sense of shear induced by the faulting was opposite to that induced by the loading frame. Two distinct flexures developed, apparently simultaneously; a short, right-lateral kink band over the fault and a long, left-lateral kink band nearby (Fig. 5C). Kink bands could not be produced in the multilayers subjected solely to faulting nor to layer-parallel shear. The layer-parallel shortening was clearly required for kink

Figure 5. Monoclinal kink bands developed in thin rubber strips under plane-strain conditions. The rubber strips are unlubricated and therefore have frictional contacts. Solid arrows indicate layer-parallel shortening; half arrows indicate shear, and *f* indicates a fault introduced by displacing a short segment of the boundary of the apparatus. (A) Layers subjected to layer-parallel shortening and layer-parallel shear. A series of monoclinal kink bands developed. (B) Same conditions as in (A), except that a fault was introduced in the boundary. The shear produced by the fault, *f*, of same sense as the general layer-parallel shear. (C) Same conditions as in (B), except the shear along the fault was of opposite sense to the general layer-parallel shear. A local monocline induced by the fault triggered a through-going monocline of the opposite sense.

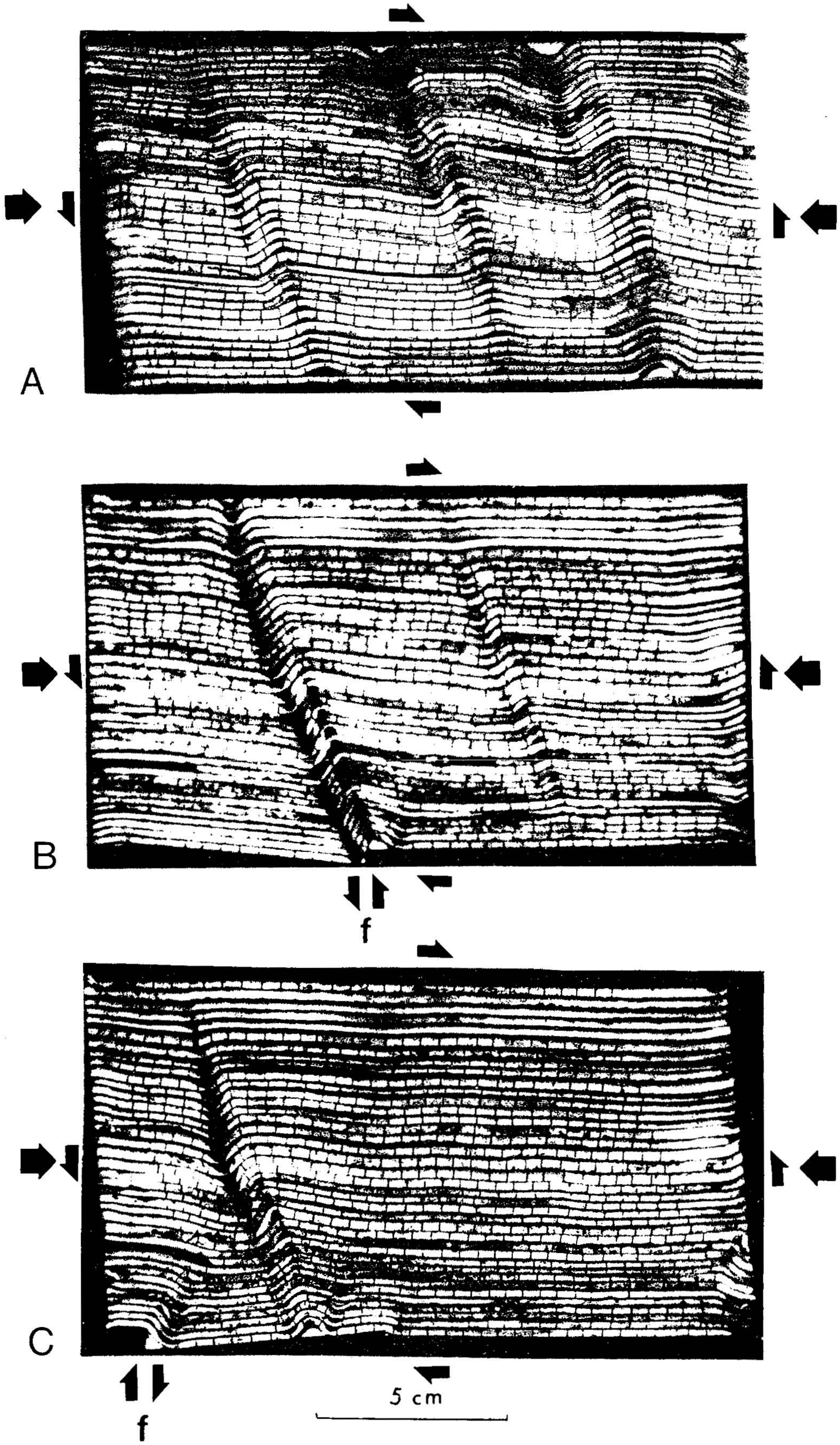
A
B
f
C
f
5 cm

folding. Further, the fault acted as a trigger to the production of the monoclinal kink bands and as a source of shear stress within the multilayer, tending to favor monoclinal kinking.

Elsewhere we have presented analyses that distinguish conditions of repetitive, sinusoidal folding from conditions of localized, kink folding (Honea and Johnson, 1976; Reches and Johnson, 1976; Johnson, 1977). The same analyses distinguish between conditions that favor the buckling mode and conditions that favor the kinking mode of monocline formation. Briefly, the kinking mode of monocline formation is favored if the moduli of layers within a sedimentary sequence are similar, if the layers are thin, and if there is layer-parallel shear. If the contrast in moduli is high, or if the contacts between layers are virtually frictionless, the buckling mode of monoclinal kinking is favored. For example, if the contrast in moduli is high, the multilayer tends to buckle with relatively high amplitudes before local slippage can occur to produce the kink form.

The kinking mode in its pure form is characterized by hinge zones where layers are bent and by limbs along which unstable yielding of contacts is the primary process. The hinges may become unstable and yield plastically or fracture if bending becomes severe. Thus, the hinges might be loci of faulting as the kink band amplified (Fig. 1A). The width of the kink band is determined largely by the bending resistance of the layers so that the thicker the layers, the wider the kink band (Honea and Johnson, 1976).

METHODS AND RESULTS OF ANALYSES

Monoclinal flexures will be idealized by simple mechanical models in order to analyze conditions that could lead to the development of such structures. Nevertheless, the models are general enough to contain many of the mechanical characteristics of deforming sedimentary sequences.

Two of the special cases of the general model, drape folding and buckling, comprise a multilayer of homogeneous, incompressible, elastic or viscous layers with different rheological properties (Fig. 2). The layers may be bonded to each other or they may have frictionless contacts and may have the same or different rheological properties. The multilayer may be subjected to both displacement and stress boundary conditions (Fig. 2). Infinitesimal plane strain is assumed.

We analyze the deformation of multilayers using methods of continuum mechanics (Apps. 1, 2). These methods provide the necessary tools for analyzing low limb-dip folding of a wide variety of materials, including linear elastic and viscous, power-law elastic and viscous, and nonlinear elastic (Fletcher, 1974; Johnson, 1977, chap. 10). We will, however, present solutions only for simple multilayers comprised of homogeneous, linear incompressible elastic or viscous material. Effects of gravity have been excluded in the particular solutions presented here, but are included in the general solution (App. 1) and will be discussed below. The reasons for making these simplifying assumptions are brevity, clarity, and we do not know the rheological properties of the rocks involved in monocline formation. Nevertheless, results of previous studies of folding indicate that the results derived from the simple models studied here are qualitatively valid for many types of rheological behavior.

An important question is the nature of the contacts between the layers in the multilayer. In natural rock sequences, the contacts are probably frictional, so that slip between the layers occurs only when the shear stresses along the contact overcome the frictional resistance. However, the solution for a multilayer with frictional contacts is complex and not available, and therefore we solve two special cases: bonded contacts and frictionless contacts.

In the analysis of kinking we consider layered media with frictional contacts between layers so that slip along the contacts occurs only when the frictional resistance is overcome. We assume finite plane strain, and slopes of layers may exceed 60° or 70° (Reches and Johnson, 1976).

RESULTS OF THE THEORETICAL ANALYSES

Drape Folding

The displacements and strains within a multilayer, produced by displacement along a vertical fault at its base (Fig. 3B), can be calculated from the solutions presented in Appendix 2. We discuss two cases of drape folding:

1. Drape folding of a multilayer with bonded contacts between the layers. There are five layers of the same thickness, three stiff and two soft. The ratio of moduli of stiff to soft layers is five. The top surface of the multilayer is stress-free (Fig. 6).

2. Drape folding of a multilayer with frictionless contacts between the layers. There are five layers of the same thickness and the same modulus (Fig. 7).

The methods of calculation are outlined in Appendix 2.

The theoretical distributions of infinitesimal displacements and strains of a drape fold in a multilayer are presented in Figures 6 and 7. The displacements are exaggerated by three orders of magnitude. We shall examine four aspects of the distribution of displacements and strains in a drape fold: the profile, the variations of curvature, the variations of displacement, and the orientation of strain axes.

Bonded Contacts. Let us discuss these features in detail for a multilayer with bonded contacts (Fig. 6).

Profile. The profile of the drape fold is a simple monoclinal form with open anticlinal and synclinal bends.

Variations in Curvature. At low levels the displacements are concentrated in a narrow zone of high curvature, whereas at high levels the displacements occur in a wide zone of low curvature (Fig. 6A). In the extreme case of a very thick multilayer, the upper surface is deflected into an open curve, whereas the lower surface is displaced by a vertical fault (Sanford, 1959).

Variations of Displacements. The vertical displacement, V, of a point on the upper surface of a drape fold (Fig. 6A) is always equal to or smaller than the vertical displacement of a point with the same x-coordinate on the base. The decrease of vertical displacement up-section was demonstrated for a single layer by Sanford (1959, Fig. 8).

Variations of the Orientation of Strain Axes. The orientation of the axes of maximum shortening is plotted in Figure 6B. Continuous strain trajectories were not plotted, because the orientation of the maximum shortening changes at the contacts between layers. The strain axes in the lower layer or two are scattered; however, the strain axes above form a clear pattern. According to orientations of strain axes, one can divide the drape fold into three zones: downthrown zone in which shortening is subparallel to layering, upthrown zone in which extension is subparallel to layering, and central zone in which simple shear is subparallel to layering (Fig. 6B). Sanford (1959) derived similar results for a single layer.

Multilayers with Frictionless Contacts. The results of the analysis of a multilayer with five thick layers of the same rheology and frictionless contacts are presented in Figure 7. The main features of the drape folding of this multilayer are as follows (Fig. 7):

Profile. The profile of the flexure is of a simple monocline with open anticlinal and synclinal bends.

Variations of Curvature. The flexure at depth is narrower than the flexure at upper levels.

Zones of Layer-parallel Shortening and Layer-parallel Extension. These zones are evident in every layer (Fig. 7B). The corresponding neutral surfaces develop similarly to those in a bending plate.

The general profile and the variations of curvature are similar in drape folding of a multilayer with frictionless contacts and in the drape folding of a multilayer with bonded contacts (Figs. 6A, 7A). However, the patterns of strain axes differ in the two cases (Figs. 6B, 7B).

A drape fold in a multilayer with frictional contacts probably has the same general shape as the two cases described above, but it probably has a more complicated strain distribution. Where there has been slippage, one expects a neutral surface in many layers. Where there has been no slippage, one expects extension

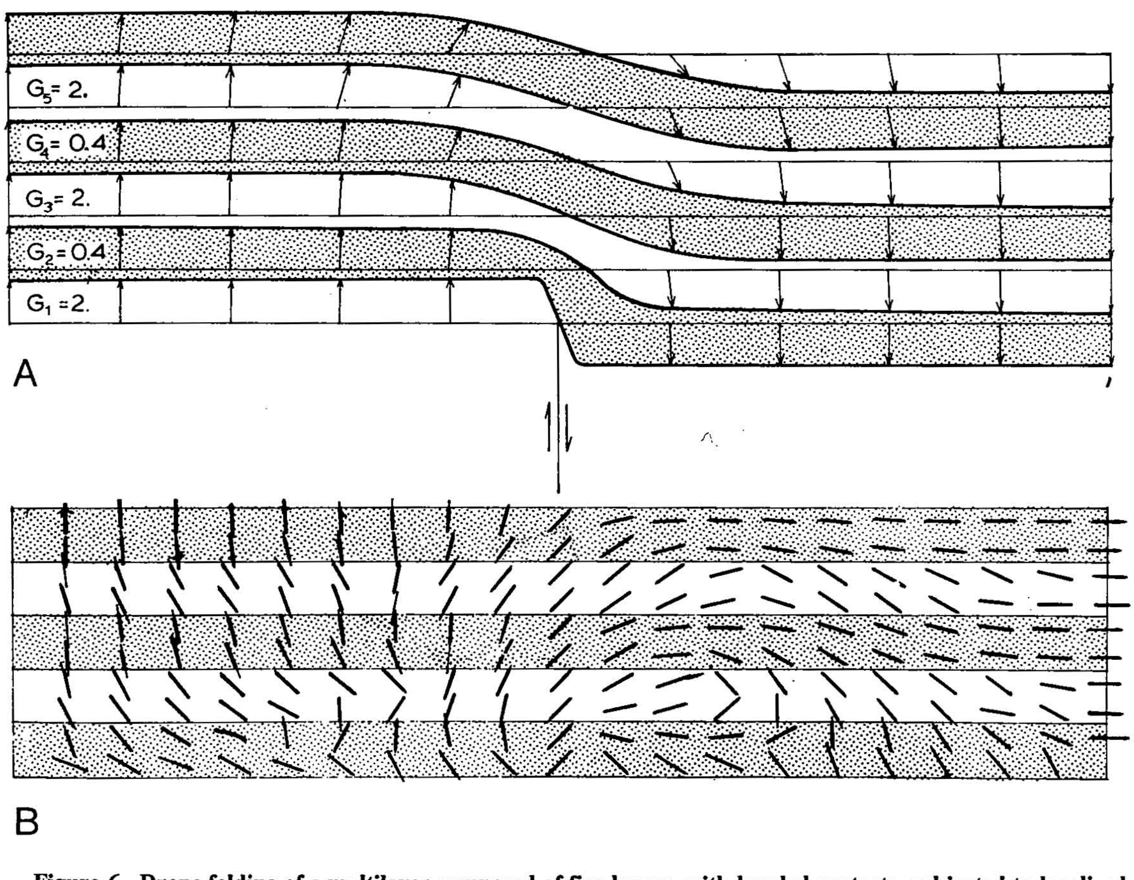

Figure 6. Drape folding of a multilayer composed of five layers, with bonded contacts, subjected to localized vertical displacements at its base. The displacements and strain orientations were calculated for an incompressible, linear multilayer (Apps. 1, 2). Shear moduli, $G_1, \ldots, G_5$, indicated on layers in their original positions. Stippled layers are the stiff layers in their deformed positions. (A) Displacements of contacts between layers. All displacements are exaggerated by three orders of magnitude. (B) Orientations of the axis of maximum shortening in the passively folded multilayer in the undeformed configuration. The orientations of shortening axes vary smoothly with position within layers, but change abruptly at contacts between layers with different properties.

or shortening within individual layers, depending upon their level within the large structure. Therefore, it is impossible to predict accurately the strain distribution within a multilayer in which contact strength has been overcome locally; however, one can conclude that zones of both layer-parallel extension and layer-parallel shortening will develop within all types of drape folds.

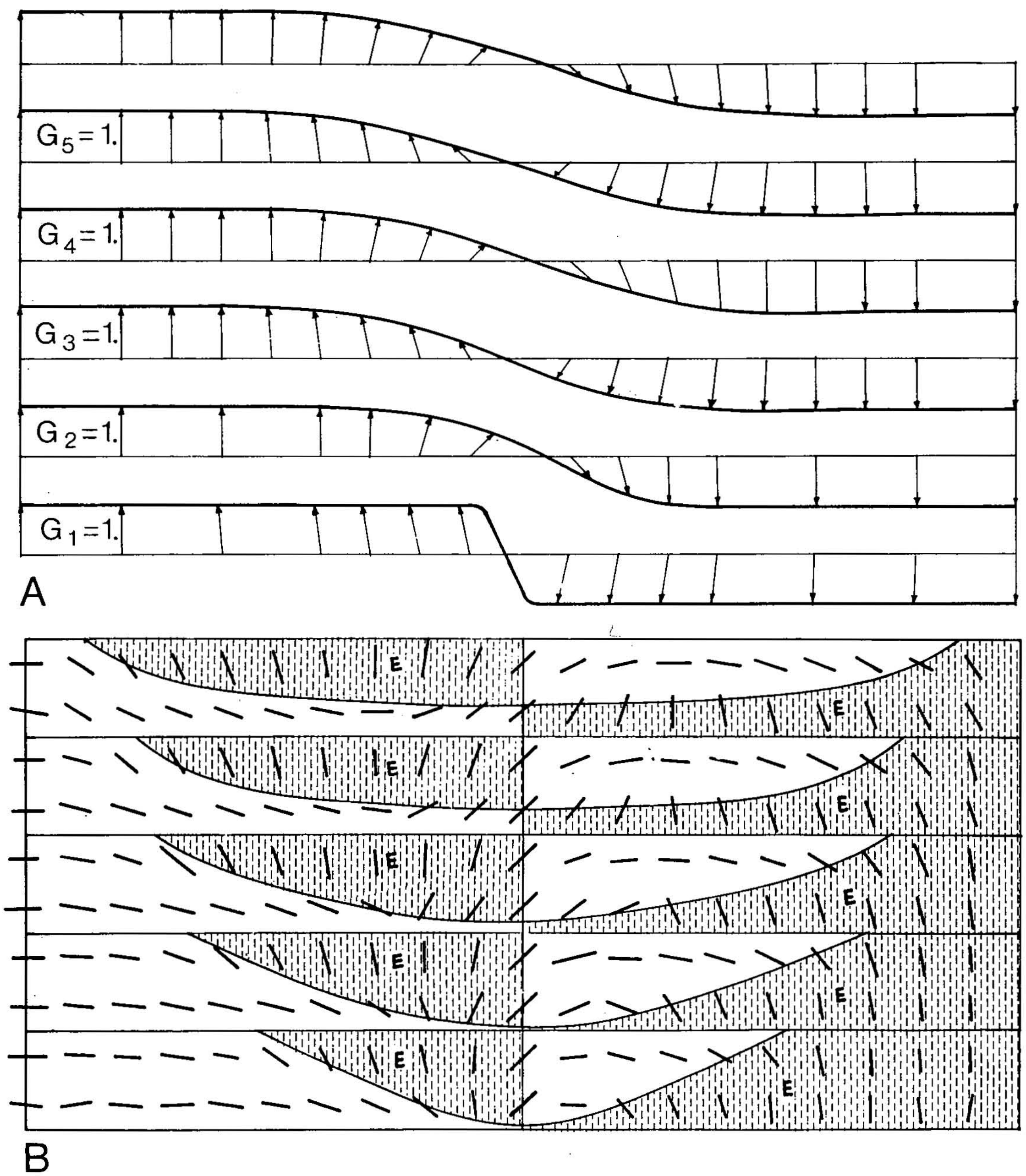

Figure 7. Drape folding of a multilayer composed of five layers with the same rheology, but with frictionless contacts. The multilayer is subjected to vertical displacement at its base. The calculations of the displacements and strain orientations are presented in Appendixes 1 and 2. (A) Displacements of contacts between layers. All displacements are exaggerated by three orders of magnitude. (B) Orientations of the axes of maximum shortening in the passively folded multilayer in the undeformed configuration. The principal strain axes are normal to all contacts between the layers. Stippled zones and the symbol *E* indicate areas of layer-parallel extension.

Combination of Buckling and Displacement of Lower Boundary of a Multilayer

The next step toward analysis of the general model of monoclinal folding is to consider both layer-parallel shortening and displacement of the base of the multilayer. The layer-parallel shortening can result in buckling in the sense that amplitudes of initial deflections become selectively amplified. In the general model we imagine the displacement of the base of the multilayer and the shortening to be simultaneous processes so that they interact with each other to produce the final monocline. However, our theory is linearized, so that we approximate the results of the simultaneous processes by applying the processes sequentially. First, we determine displacements within the multilayer as a result of drape folding

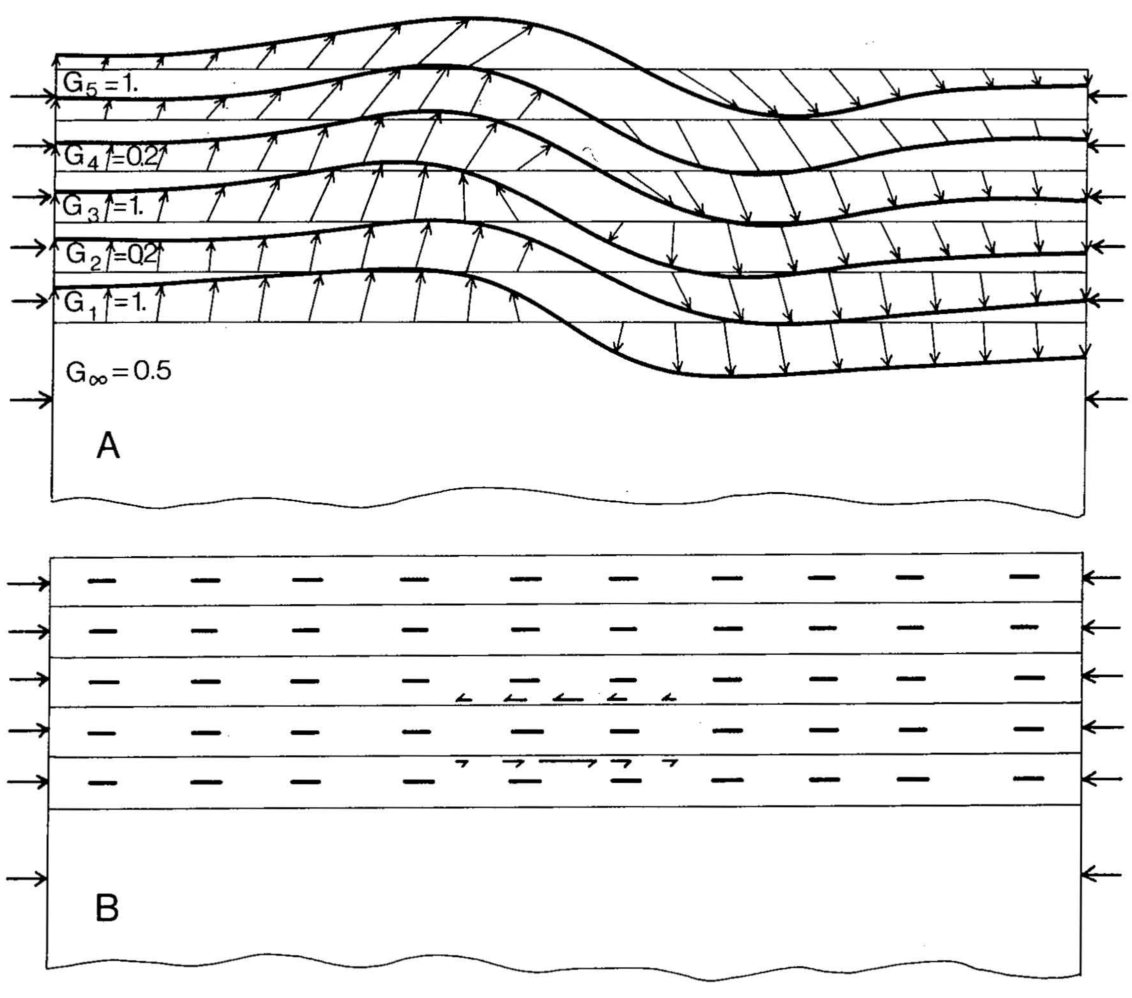

Figure 8. Buckling of a multilayer composed of five layers with bonded contacts. The lower medium is as stiff as the mean stiffness of the multilayer. The multilayer was first passively folded into a very low amplitude monoclinal flexure similar to that shown in Figure 5. Then the initial monoclinal flexure was buckled as a result of layer-parallel shortening of 0.001. Only the strains and displacements due to the buckling stage are plotted. (A) Displacements of contacts between layers. Displacements are exaggerated by three orders of magnitude. (B) Orientations of the axes of maximum shortening in the buckled monoclinal flexure in the undeformed configuration. The axes of the total strain, uniform and incremental (App. 1), are plotted. The small arrows marked above and below layer 2 indicate the relative magnitude and sense of the incremental layer-parallel shear (σ_{ns} in Apps. 1, 2).

in response to displacements along the base of the multilayer. Then we treat these displacements as *initial* displacements which become amplified as a result of layer-parallel shortening (App. 2). We should note that buckling is impossible in perfectly flat layers of viscous materials and virtually impossible in perfectly flat layers of elastic materials. Thus, we use the displacements due to drape folding to select the form of the initial displacements of interfaces between layers.

Choice of Multilayer. A single layer embedded in an infinite soft medium has one dominant wavelength which is determined approximately by equation (1). However, multilayers composed of many layers with arbitrary thicknesses and moduli can have several dominant wavelengths. We have chosen to analyze simple multilayers of alternating soft and stiff layers rather than complicated multilayers. The multilayer behaves much as the single layer described in earlier pages, in that the initial monocline will be amplified during shortening only in a multilayer which has a dominant wavelength on the order of the width of the initial monocline. Other multilayers also buckle, but into shorter or longer wave forms. The infinite lower medium (Fig. 8) below the multilayer has an important effect on the dominant wavelength. If the lower medium is stiff relative to the multilayer above, the dominant wavelengths will be short (Johnson, 1977, chap. 11) and may be less than the width of the monocline. On the other hand, if the lower medium is very soft, the dominant wavelengths may be larger than the width of the monocline. We arbitrarily chose a multilayer with alternating soft and stiff layers with bonded contacts overlying a lower medium with a shear modulus approximately equal to the mean shear modulus of the multilayer (Fig. 8).

The analysis of buckling of a multilayer with frictionless contacts indicates that the dominant wavelength depends mainly on the thickness of the layers and is virtually independent of the modulus of the lower medium if the modulus of the medium is greater than the modulus of the layers (Johnson and Page, 1976, Fig. 12).

We studied several multilayers with bonded contacts and with frictionless contacts and found that monoclines will be amplified in multilayers with a limited range of properties if contacts are bonded but will be amplified in most multilayers with frictionless contacts.

Results. The theoretical distribution of displacements and strains due to buckling of a multilayer are presented in Figures 8 and 9. In our calculations, the multilayer is first passively folded by a small displacement along a vertical fault at its base (Fig. 6). Then the initially deflected multilayer is subjected to layer-parallel shortening of magnitude 10^{-3}, which causes it to buckle. Methods of calculation and boundary conditions are presented in Appendix 2. We will again discuss the distribution of the deformation rather than the absolute magnitudes of the strains and displacements. We will discuss in detail the buckling of a multilayer with bonded contacts (Fig. 8), and we will discuss briefly the buckling of a multilayer with frictionless contacts (Fig. 9).

Bonded Contacts.

Profile. The profile of a monocline formed by buckling is characterized by a monoclinal flexure, with associated anticline and syncline (Fig. 8). The anticline and syncline replace the anticlinal bend and synclinal bend of the drape fold (Fig. 6). A similar profile was obtained in experiments involving a single rubber layer in gelatin (Fig. 4A).

Variation of Curvature. The profiles of the different layers in the buckled monocline are similar to each other (Fig. 8). One can, however, see a slight difference between the profile of the base of layer 3, for example, and the profile of the top of layer 3. This minor variation is the result of incremental shear which develops during the buckling (App. 1). In general, however, the layers maintain similar profiles at all levels.

Variations of Displacements. The vertical displacements of the layers in a buckled monocline increase up-section. Thus, the displacement, V, of a point at the top of the multilayer in the anticlinal bend is always equal to or larger than the displacement at the same distance, X, at the base of the multilayer (Fig. 8). This result is expected because the upper surface of the multilayer does not resist vertical displacement of the multilayer, whereas the lower surface in contact with the infinite medium does.

Variation of Orientation of the Strain Axes. The strains in the buckled monocline can be separated into uniform horizontal strain which causes the buckling and incremental strain which results from the buckling (App. 1). The total strain is the sum of the uniform strain and the incremental strain. However, the incremental strain is two to three orders of magnitude smaller than the uniform strain; therefore,

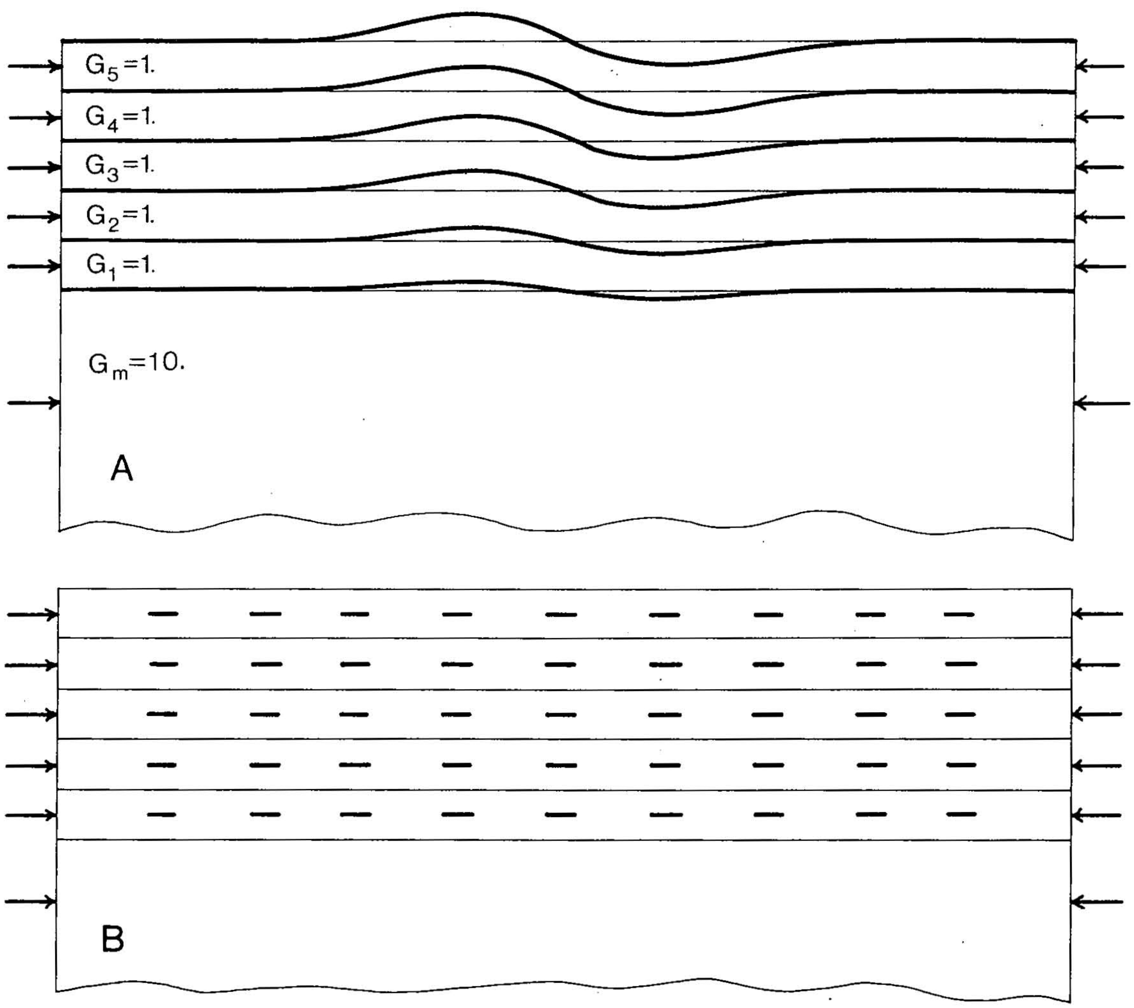

Figure 9. Buckling of a multilayer composed of five identical layers with frictionless contacts. The lower medium is ten times stiffer than the layers above. The multilayer was first passively folded as in Figure 6. Then the multilayer was buckled as a result of layer-parallel shortening of 0.001. Only the strains and displacements due to buckling processes are plotted. (A) Displacements of contacts between layers. Displacements are exaggerated by three orders of magnitude. (B) Orientations of the axes of maximum shortening in the buckled monoclinal flexure. The axes of the total strain, uniform and incremental (App. 1), are plotted.

the total strain in the monocline is essentially uniform layer-parallel shortening (Fig. 8B) for low-amplitude flexures.

Multilayer with Frictionless Contacts. The results of the buckling of a multilayer with frictionless contacts, due to layer-parallel shortening, are shown in Figure 9. The conditions assumed in the analysis differ from those for bonded layers in two respects: First, we assume the same properties for all five layers. Second, the lower medium is ten times stiffer than the layers above, whereas, for the multilayer with bonded contacts, the modulus of the lower medium was approximately equal to the average modulus of the layers above.

The most striking feature of the buckling of a multilayer with frictionless contacts is the strong amplification of the monoclinal flexure up-section. The vertical displacement at the top of the fold in Figure 9 is about ten times greater than the vertical displacement at the base of the multilayer. The cause of this difference in amplification is the stiff lower medium which is not able to buckle similarly to the multilayer, whereas the lack of confinement of the surface of the multilayer enables the monocline to be amplified up-section.

The monoclinal flexures we analyzed were initiated and localized by draping which deformed the multilayer before layer-parallel shortening. We presented orientations of strains, however, produced solely by the layer-parallel shortening and buckling. Zones of layer-parallel extension develop in the anticlinal bend of a drape fold (Figs. 6, 7), whereas layer-parallel compression prevails throughout the buckled monoclines. Therefore, it is important to superimpose the strains produced by the draping upon the strains produced by the folding. Unfortunately, there is no general relation between these strains because the amount of displacement along the fault during draping is unrelated to the amount of layer-parallel compression. We can, however, report the results of the superposition of strains for two multilayers analyzed here (Figs. 6, 8). The displacement of 1% of the total thickness of the bonded multilayer along a vertical fault (Fig. 6) produces maximum layer-parallel extension of about 0.7% in the upthrown block of the multilayer. Therefore, shortening of the multilayer by about 0.7% would eliminate the extension in the upthrown block due to draping.

Effects of Gravity

The general model of monoclinal flexuring includes the effects of gravity on stresses and displacements within a multilayer. We did not include effects of gravity in the solutions presented in earlier pages because the effects are negligible. We can demonstrate this by calculating the stresses and displacements in a homogeneous half space, the surface of which is deflected into a sinusoidal wave. For small deflections, where the amplitude-to-wavelength ratio (h/L) is much less than unity, the deformation of the half space can be evaluated with equations (21a–21h), Appendix 2. The displacements at the surface resulting from gravity tend to lower the elevated areas and to elevate the low areas, as would be expected.

Solution of equations (21a–21h) for an elastic half space shows that the surface displacements due to gravity are proportional to a parameter D,

$$D = \rho g/(4\pi G),$$

where ρ is density, g is acceleration of gravity, and G is the shear modulus. In order to estimate the maximum magnitude of the displacement, we use densities and shear moduli determined for rocks. A representative value for D for limestone, sandstone, shale, granite, and basalt, according to data presented by Clark (1966), is 10^{-9} cm^{-1}. Using this value and choosing a surface deflection of

$$h = 0.01\,L,$$

we compute the maximum displacement of the surface due to gravity

$$V_{\max} = 10^{-3}\,h.$$

That is, the correction to the displacements at the ground surface, where the correction is maximal, is about three orders of magnitude less than the displacement, h, of the surface due to draping or buckling. These corrections are clearly negligible for low-amplitude deformations such as those we consider in our linearized analyses.

Now let us consider the stresses. Stresses induced by gravity in a multilayer can be divided into two parts. One part is a result of the differences in altitude of different parts of the ground surface. The maximum difference of these stresses within the multilayer is proportional to the amplitude of the surface deflection and is therefore small if the deflection is small, as in our first-order analysis. The other part of the gravity stresses is hydrostatic and is directly proportional to the depth below the surface. This hydrostatic stress can be superimposed on the stresses produced by folding. Further, the hydrostatic stress produces strains in a compressible material, and these strains can be superimposed on the strains produced by folding. In incompressible materials, which we are considering here, hydrostatic pressure produces no strain, so there would be no correction to the strains computed by ignoring gravity.

Therefore, gravity has negligible effects on the strain and displacement distributions reported in previous pages, primarily because the deformations are small. An analysis of finite deformations, of course, must include effects of gravity.

DISCUSSION

The ultimate objective of our study is to identify general processes of monoclinal flexuring, including those responsible for the large monoclines on the Colorado Plateau and those responsible for monoclinal kink bands in foliated materials. A general model that we believe to include most of the processes is partly illustrated in Figure 2. The features of the general model not illustrated are reviewed in the discussion accompanying Figure 2. Not all possible conditions of the general model will lead to a flexure of monoclinal form, however, as has been indicated already by the analyses presented in earlier pages. Further analysis is required to specify those conditions that will; one based on finite-element techniques, using nonlinear, elastic-plastic materials, is in progress.

Perhaps the greatest value of the process of developing a general model is the selection of parameters that must be included in a comprehensive analysis. We have shown, through study of three special cases which we have loosely called "kinking," "drape folding," and "buckling," that a wide variety of conditions can be responsbile for monoclinal folding, even in simple linear materials. Clearly a notion that all monoclines are drape folds would be impossible to defend.

In our attempt to develop a general model of monoclinal flexuring, we have performed theoretical and experimental analyses of monoclinal kink bands in foliated materials (Reches and Johnson, 1976), we have made a detailed structural analysis of the Palisades monocline (Reches, this volume), and we have examined two special cases of our general model of monocline formation in previous pages.

A summary of the general results of the study of the theoretical models is presented in Table 2.

Limitations of the Theoretical Analyses

We will re-examine some of the field observations made in the Palisades monocline, as well as those made elsewhere by other investigators, and attempt to explain some of the observations in terms of the theoretical and experimental analyses. However, in order to compare the theoretical and field observations, we must know the limitations of the theory.

The theoretical analysis of the buckling mode of monocline formation is qualitatively valid for materials with a wide range of properties, including linear elastic or viscous, power-law elastic or viscous, and nonlinear elastic (Fletcher, 1974; Johnson, 1977, chap. 10). The analysis of drape folding is qualitatively valid for compressible or incompressible elastic or viscous materials. The specific results are valid only for incompressible elastic or viscous materials. However, the results

TABLE 2. SUMMARY OF TYPICAL FEATURES OF THREE SPECIAL MODELS OF MONOCLINAL FLEXURING ACCORDING TO ANALYSIS

Contacts between layers	Mode of monoclinal flexuring		
	Drape folding	Buckling	Kinking
Bonded contacts	1. Simple monoclinal flexure with anticlinal and synclinal bends	1. Monoclinal flexure with associated anticline and syncline	Kinking not possible
	2. Decrease of curvature of profile up-section	2. Increase, decrease, or constant curvature up-section, depending on properties of multilayer	
	3. Decrease of vertical displacement up-section	3. Constant or increase of vertical displacement up-section in the anticlinal zone	
	4. Zones dominated by layer-parallel shortening, extension, or shear	4. Layer-parallel shortening dominates at all levels	
Yielding contacts	Solution not available	Solution not available	1. Profile comprised of straight limb and tight hinge zones 2. Constant profile 3. Constant displacement 4. Yielding in hinges
Frictionless contacts	1. Simple flexure	1. Flexure with associated anticline and syncline	Kinking not possible
	2. Decrease of curvature up-section	2. Curvature generally increases up-section	
	3. Constant vertical displacement up-section	3. Increase of vertical displacement up-section in anticlinal zone	
	4. Every layer contains zones of shortening, shear and extension	4. Layer-parallel shortening at all levels	

Note: Summary of Figures 6, 7, 8, and 9 and Reches and Johnson (1976).

are presented in terms of nondimensional parameters such as relative displacements, strain or strain rates, and relative moduli or viscosity coefficients, so we consider the specific theoretical results presented here to be sufficiently general to elucidate the characteristics of the three special cases of the general model of monocline formation. There are, though, several important limitations in the analyses:

1. Rocks within certain parts of monoclines have been subjected to finite deformations and rotations, whereas the theories of drape folding and buckling discussed in previous pages assume infinitesimal strains and rotations. Thus, the theory is valid only for the inception of monocline development. The limitation of smallness of deformations is necessary in order to linearize the basic equations used to describe the deformations; also, it allows us to generalize the solutions to include certain aspects of power-law or other nonlinear rheological models.

The theory of kink folding, unlike the theories of drape folding and buckling, is not restricted to small deformations and rotations. As shown elsewhere (Reches and Johnson, 1976), we can investigate yielding instabilities of contacts between layers regardless of the slope angles of layers, and the yielding of contacts appears to control the high-amplitude growth of conjugate and monoclinal kink bands, including the orientations of kink bands and the locking angles of layering within kink bands. Thus, the theory of kinking incorporates certain nonlinearities that the other theories cannot incorporate, but the theory of kinking is so elementary that it cannot describe displacements and strain patterns in the way that the other theories can.

There is evidence derived from experiments and high-amplitude folding theory that sizes of folds are largely controlled by sizes of the first-formed folds, which we can study with the linearized theory presented here. The linearized theory apparently closely describes deformations within folding layers where maximum slopes of layering are less than 10° to 15° (Sherwin and Chapple, 1968; Dietrich and Carter, 1969; Hudleston and Stephansson, 1973). Therefore, it is quite likely that the linearized theories of monocline formation are valid for similar maximum slopes of layers, because the sources of error are the same in the theories. Hudleston (1973) has shown experimentally that wavelength selection and layer-parallel shortening are active primarily during early stages of growth of high-amplitude folds. Sherwin and Chapple (1968) and others have deduced useful information from high-amplitude folds by using infinitesimal strain theory and comparing theoretical wavelengths with arc lengths measured in the field.

On this basis we suggest that our theoretical analysis of drape folding and buckling is applicable to monoclinal flexures sloping up to 10° to 15° and may explain certain features of even steeper monoclinal flexures.

2. Idealized material properties of contacts between layers, such as bonded contacts, free-slip of contacts, or contacts with finite strength, were assumed in order to allow theoretical analysis. None of these idealized conditions corresponds with actual field conditions, of course, but they should allow us to understand some aspects of field conditions. Even though the cases of bonded contacts and free slip are end members of resistance to slip along layers, the two cases do not represent end members of deformations of contacts. Thus, if we derive the shape of a fold in a multilayer with bonded contacts and the shape of a fold in the same multilayer with frictionless contacts, we still cannot predict the shape of the fold in the same multilayer having finite contact strength. The reason is that localized slippage of contacts can fundamentally change the fold form. Indeed, it is precisely this condition that allowed us to develop a theoretical model for the isolated kink form (Honea and Johnson, 1976).

3. The multilayers we have selected to analyze are highly idealized, whereas

multilayers in the field are difficult to define. In our study of kinking we have assumed that each layer has the same rheological and dimensional properties, a condition closely approached in the experiments but never achieved in the field. In our study of buckling and passive folding, we have also selected relatively simple multilayers. It is no simple matter to identify structural units in the field (Chapple and Spang, 1974; Johnson and Page, 1976), so it is difficult to select realistic multilayers in terms of either rheological or dimensional properties. Detailed comparisons of theoretical results and field observations will require careful estimations of field conditions.

4. The analyses cannot account for some important behaviors associated with nonlinear rheologic properties or with faulting. We believe that the location and orientation of major faults within monoclines cannot be deduced from the analyses of buckling, drape folding, or kinking. One reason is that large deformations generally cannot be incorporated in the theory. Another is that the stress and strain distributions within multilayers may change considerably due to the existence of a large fault, so that, as soon as the fault begins to develop and propagate, the stresses become redistributed and must be recalculated. Analyses of this type are not yet available. Our analyses definitely are valid only for continuous and unfaulted monoclinal flexures. Small faults, which disrupt the stress distribution only locally, however, probably have minor effect on the gross deformation of a multilayer so that a multilayer containing small faults probably can be considered to be continuous.

Field Examples

Palisades Monocline. The Palisades monocline, which was described in a companion paper (Reches, this volume), will be analyzed by means of the general model of monoclinal flexuring. We shall review a few of its salient features and then compare these features with those of the idealized monoclines.

The Palisades monocline is a branch of the East Kaibab monocline in the eastern part of Grand Canyon National Park. It is nearly perfectly exposed in Palisades Creek, so that an accurate structural cross section could be prepared (Fig. 10). First let us consider the gross form of the monocline. The structure can be divided into three levels: a lower level that includes the vertical fault and steep layers in the adjacent synclinal zone; a central level of continuous but tight flexuring; and an upper level of open flexuring (Fig. 10). The lower, faulted level cannot be compared with our theoretical models because our models were derived for nonfaulted monoclines, so we are unable to discuss it.

The profiles of contacts between rock units within the upper two levels are characterized by a transition from a tight monocline, with layers dipping up to 90° in the Bright Angel Shale, Muav and Temple Butte limestones, into an open monocline with maximum dips of 20° to 25° in the Redwall Limestone and in units above (Reches, this volume). The anticlinal bend of the monocline has a radius of curvature of about 10 m, and the synclinal bend has a radius of curvature of about 150 m at the base of the Bright Angel Shale (Fig. 10), whereas both the anticlinal and synclinal bends have radii of curvature of about 4 km at the level of the Kaibab Limestone (unit P in Fig. 10).

The difference of structural levels across the base of the monocline is about 250 m, and the structural difference is constant or slightly decreasing up-section.

Thus, the profiles at various levels within the Palisades monocline are similar to those predicted by the drape folding case of our general model of monoclinal formation (Table 2). The relatively straight limb of the monocline in the central level, within the Bright Angel Shale and Muav Limestone, resembles a kink fold, but the proximity of this part of the structure to the large fault makes such an interpretation tenuous. We can state that there is no clear evidence for an anticline associated with the anticlinal bend or a syncline associated with the synclinal bend, as would be expected if much of the growth of the monocline were due to the buckling mode. Further, there is no evidence for increasing structural relief across the monocline up-section, as would be expected if buckling were strong.

On the other hand, the internal structures of the Palisades monocline do not correspond with those expected in a monocline developed as a drape flexure. The internal structures and measurements of strain orientations, using petrofabric analysis of carbonate rocks in the area, were described at length in a companion paper (Reches, this volume). Nearly all the measurements of small faults, small folds, twinning of calcite, and changes of thickness of units indicate maximum compression subparallel to layering at all levels within the monocline. These results are consistent with those expected in a monocline formed according to the idealized buckling or kinking mode but not the drape folding mode. If the Palisades monocline had formed via the drape folding mode, we would expect zones of layer-parallel extension in certain parts of the monocline, depending upon the properties of contacts between layers. For example, if the layers were bonded, we would expect marked layer-parallel extension in the anticlinal zone of the Palisades monocline, but we found evidence for compression there (Fig. 10).

Thus, analysis of the gross shape and the internal deformation patterns of the Palisades monocline leads us to the conclusion that the monocline formed as a

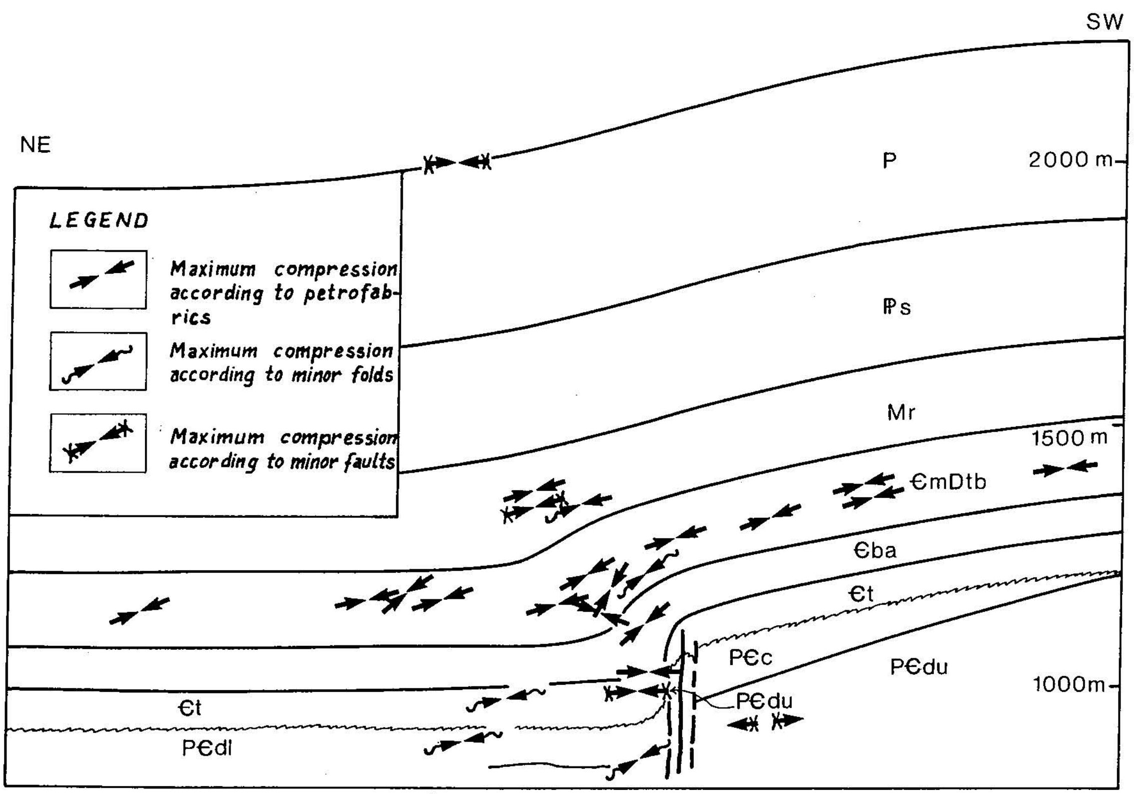

Figure 10. Vertical cross section of the Palisades monocline, Grand Canyon, Arizona. The solid arrows show the orientation of axes of maximum compression as interpreted from analyses of small structures and petrofabrics. Stratigraphic units range from Dox Formation of the Precambrian to Kaibab Limestone of the Permian (after Reches, this volume).

result of uplift along the Palisades Fault at its base, along with layer-parallel compression. The results do not correspond clearly with any of our three special cases of the general model of monocline formation. Without specific knowledge of the rheological and dimensional properties of structural units within the monocline, we are unable to determine the relative contributions of vertical displacements along the base of the monocline and buckling of layers within the monocline to the development of its present shape.

In a companion paper (Reches, this volume) we showed that the direction of maximum compression was oblique to the axis of the monocline, and one might well wonder if this is the reason there is no evidence for the buckling mode in the general form of the monocline. We think not. Analysis of three-dimensional folding based on plate theory, either for single layers or multilayers (Johnson and Page, 1976), indicates that the components of stress that are important to folding depend upon the shape of the perturbation to be amplified by buckling. Thus, the driving term in the differential equation describing the equilibrium of a layered system is (Johnson and Page, 1976, equation 24a)

$$[S_{xx}(\partial^2 v/\partial x^2) + S_{yy}(\partial^2 v/\partial y^2)], \tag{2}$$

where x and y are horizontal axes, v is vertical displacement, and S_{xx} and S_{yy} are principal components of horizontal stresses. Let S_{xx} act normal to and S_{yy} parallel to the axis of a *cylindrical* monoclinal perturbation. The shape of the perturbation can be described in terms of a Fourier series, such as

$$v = a \sin(\ell x) + b \sin(2\ell x), \ldots, \tag{3}$$

where $a, b, \ldots,$ are coefficients and ℓ is a wave number defined as in Appendix 1. If equation (3) is substituted into equation (2), it is clear that the term involving the normal stress, S_{yy}, vanishes and only the term involving the stress, S_{xx}, normal to the axis remains. Thus, only the magnitude of the stress normal to the axis of the cylindrical perturbation is important in determining the amplification of the perturbation into a fold. Amplification of the perturbation will occur, therefore, if the axis-normal stress is compressive; it will occur even if the horizontal stresses are equal. This is merely one more example of the importance of the form of the initial perturbation on the shape of resulting folds, a concept introduced long ago by Willis (1894).

We suggest the following sequence of events during the development of the Palisades monocline. The strain field of the Laramide orogeny in the area of the Palisades monocline was dominated by subhorizontal, regional shortening. The regional trend of the shortening is unknown, but the areal trend in the vicinity of the eastern part of Grand Canyon National Park was about N65°E (Reches, this volume, Fig. 21). The branch of the Butte fault in Palisades Creek had developed during the Precambrian with a northwest trend. Its strike deviated about 70° from the axis of maximum shortening during the Laramide. The fault was unfavorably oriented relative to the directions of stresses in the sedimentary cover during the Laramide orogeny. However, the fault apparently provided a weak zone relative to blocks around it, and unknown, deep-seated processes caused large blocks of the Colorado Plateau to move vertically relative to each other. The sedimentary rocks above the fault became flexed into a monocline, apparently in response to a combination of horizontal shortening and differential vertical uplift.

Yampa Monocline. Cook and Stearns made a series of cross sections through the Yampa monocline in Dinosaur National Monument, Colorado and Utah, and mapped internal features of the monocline in some places (Cook, 1975; Cook and Stearns, 1975). We shall present some of the cross sections of the Yampa monocline and discuss its gross geometry and internal structures in terms of the theory developed here.

The Yampa monocline is about 20 km long, trends east, and has a maximum structural relief of about 500 m. A reverse fault is exposed along the eastern part of the monocline, whereas a continuous, unfaulted flexure occupies the western part of the monocline (Cook and Stearns, 1975, Fig. 1). Four cross sections of the western part of the monocline are shown in Figure 11. The most important characteristics of the monocline are

1. Small reverse and thrust faults are common within the monocline. They are particularly common in the anticlinal and synclinal bends (Fig. 11B, 11A) (Cook, 1975, Fig. 17). Intense fracturing with no clear displacement direction commonly occurs in the anticlinal and synclinal bends. Small normal faults were not observed in the Yampa monocline.

2. Thickening of the Weber Sandstone up to 50% prevails in the western part of the Yampa monocline (Fig. 11C) (Cook and Stearns, 1975, Fig. 6). At one location (Fig. 11B), "The Weber Sandstone is thinned approximately 10% normal to bedding; however, small thrust faults and shear fractures have shortened and thickened the formation perpendicular to the fold axis" (Cook and Stearns, 1975, Fig. 7).

3. The amplitude of the Yampa monocline and of neighboring monoclines within the Weber Sandstone increases up-section in some places (Cook and Stearns, 1975, Figs. 8, 9). For example, the structural relief across the monocline at the base is about half that at the top of the Weber Sandstone in one cross section (Fig. 11C).

4. The Yampa monocline is characterized in some places by blocks within which layers are straight but have different dips from layers in adjacent blocks (Fig. 11D). Fracturing is less intense within the blocks than within "hinges" between the blocks. In some places the "hinges" contain faults.

The Yampa monocline is fascinating for its variety of forms. However, all the observations seem to correlate with a mechanical model in which both vertical uplift and horizontal compression were important, as in the Palisades monocline.

Two cross sections of the Yampa monocline resemble large kink bands (Fig. 11A, 11D). In one, there is abundant evidence of layer-parallel shortening in the form of small reverse and thrust faults; the limb is quite straight and the hinges are rounded but narrow (Fig. 11A). In the other, there appear to be several limbs that are quite straight separated by very narrow hinge zones (Fig. 11D). According to our analyses, these forms require high, layer-parallel shortening and yielding of contacts between structural layers. A fault below the Weber Sandstone probably served as a trigger to the flexuring, much as in one of our experiments (Fig. 5B).

The third cross section (Fig. 11B) shows internal evidence of horizontal shortening, but the form of the flexure provides no information concerning the dominant mechanism of its formation. The anticlinal and synclinal bends and the limb are all curved. The fourth cross section (Fig. 11C) shows evidence of increase of amplitude of the flexure up-section, as in our idealized buckling mode of monoclinal flexuring.

Only the general model of monoclinal flexuring can account for the major features of the Yampa monocline that show evidence of buckling and kinking. No part of the Yampa monocline is consistent with a model of drape folding.

Experimental Monoclinal Flexuring. Some of the results of the theoretical analyses

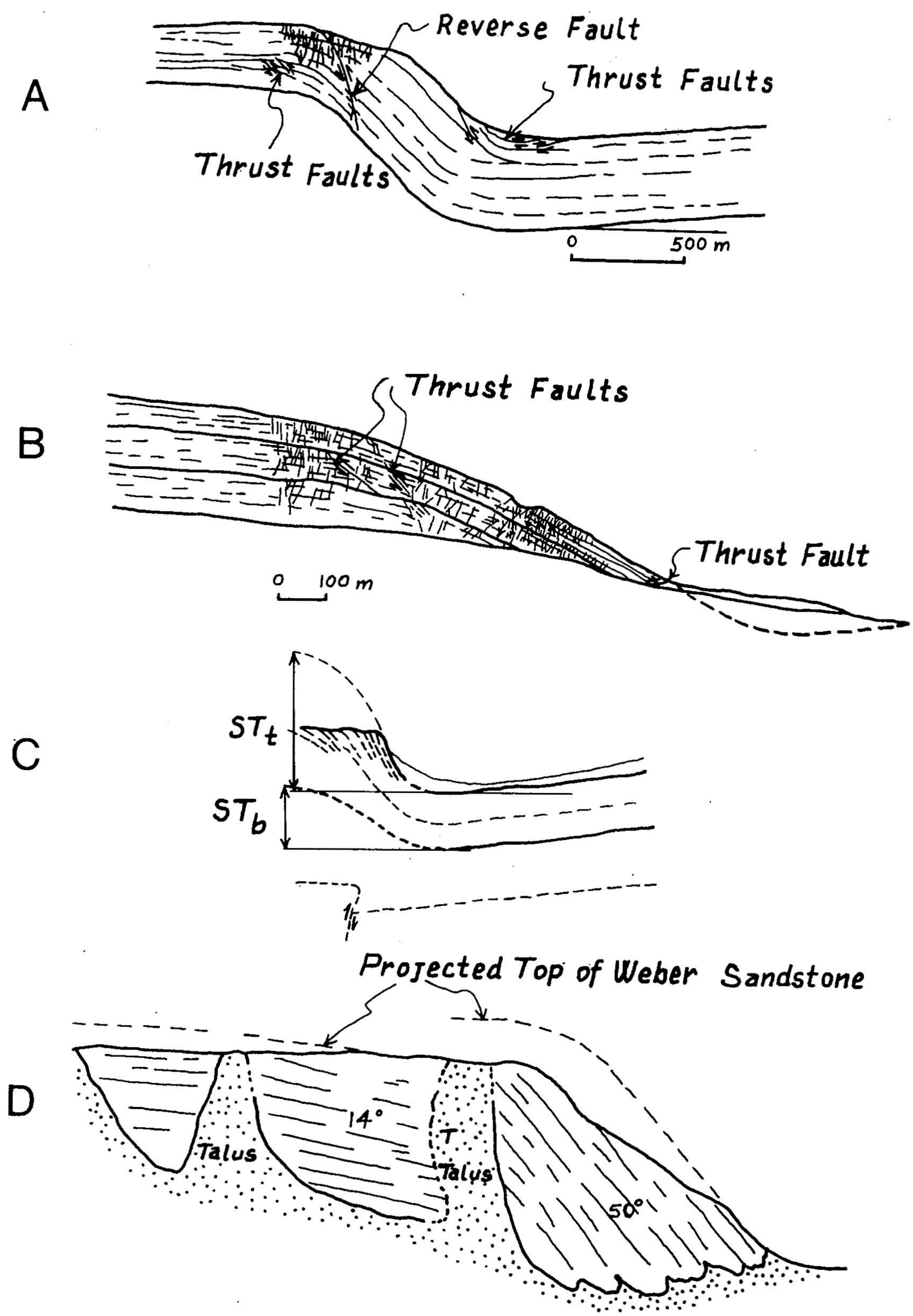

Figure 11. Vertical cross sections trending north, of the Weber Sandstone in the Yampa monocline, Dinosaur National Monument, Utah and Colorado. In *C,* ST_b and ST_t are the structural throw of the base and the top of the Weber Sandstone, respectively (after Cook, 1975; Cook and Stearns, 1975).

of monoclinal flexuring can be compared with experimental monoclines produced by Friedman, Logan, and others. Friedman and others (1976) and Logan and others (this volume) described experimental monoclinal flexures developed in multilayers comprised of sandstone and limestone, and presented distributions of strain and stress with the multilayers derived from analyses of microfractures, calcite twins, and thickening of layers. The multilayers were subjected both to confining pressure and to displacement along a fault at one side of the multilayer (Fig. 12). According to descriptions by Friedman and others (1976, p. 1053), bedding-plane slip within the multilayer was negligible. Thus, the conditions of the experiment shown in Figure 12 closely correlate with those assumed in the theoretical model of a multilayer with bonded contacts (Figs. 6, 8; Table 2). In both the experiment and the theoretical model the multilayer is simple, with alternating soft and stiff layers, and a small displacement occurs along a vertical fault.

According to Figure 12, the flexure is tight and narrow in the lower part, near the fault, and wide and open above. Also, layer-parallel extension is evident in the anticlinal bend of the experimental monocline, and layer-parallel compression is evident in the synclinal bend. The extension in the anticlinal bend is definitely inconsistent with the buckling mode of monocline formation (Fig. 8). Indeed, all the features are evident in the theoretical monoclinal flexure produced by drape folding of a multilayer with bonded contacts (Fig. 6).

CONCLUSIONS

Monoclines are generally simple-appearing structures with a single limb and smooth profile. Powell (1873) displayed usually sound physical insight when he recognized the close association of faults below and monoclinal flexures above. Further, Sanford (1959) provided a sound model of monoclinal flexuring in which the overburden is deformed passively as a result of faulting below. Thus, the model of drape folding is an attractive model of monocline formation. Yet, the simple drape-folding model cannot account for many observations made in detailed studies of monoclinal flexures. There is abundant evidence of layer-parallel shortening in anticlinal zones of many monoclines; therefore, shortening must be incorporated in a general model of monocline formation. Further, we have shown that monoclinal kink bands can develop in response to layer-parallel shortening and shear, even without the necessity of the marked local disturbance produced by displacement along a fault below (Reches and Johnson, 1976). We do not know

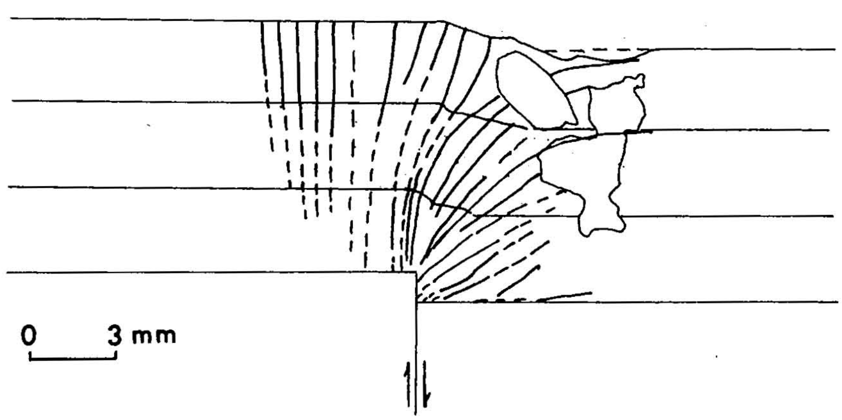

Figure 12. Map of trajectories of the maximum principal compressive stress as interpreted from orientations of faults and microfractures in an experimental passive fold. Stippled layer is sandstone; other layers are limestone (after Logan and others, this volume).

whether any large monoclines have been produced in this way, but it is possible.

We imagine that a monoclinal flexure generally initiates above a disturbance, such as a fault, an igneous intrusion, a local steepening of layers, or a buckle. Without such a disturbance, there generally is no theoretical basis for the initiation and localization of a monoclinal flexure. Our general model of monocline formation includes effects of layer-parallel shortening and shear, of vertical displacement of the base of a multilayer, and of a wide range of dimensional and rheological properties of layers as well as properties of contacts between layers. We have analyzed specific cases of the general model: drape folding, in which the disturbance at the base causes the overburden to deform passively; buckling, in which the layer-parallel shortening and the vertical uplift interact to amplify the perturbation at depth; and kinking, in which buckling and yielding instabilities result in a kink band in the overburden.

We solved some specific examples of multilayers subjected to drape folding and to buckling in order to determine the general characteristics of monoclines produced by pure forms of these processes. The characteristic features are summarized as follows:

Drape Folding

1. Monoclinal flexure is simple, with open anticlinal and synclinal bends.
2. Curvature increases downward so that monocline is tight below and open above.
3. Vertical displacement is constant or decreases up-section.
4. There are zones of layer-parallel extension and zones of layer-parallel shortening. The pattern of the zones can be complicated in irregular multilayers; however, the lack of zones of extension is incompatible with the drape-folding mechanism.

Buckling

1. Monoclinal flexure is associated with an anticline and a syncline.
2. Curvature is constant, increases or decreases up-section.
3. Vertical displacement is constant or increases up-section.
4. Layer-parallel shortening prevails at all levels (Figs. 7B, 8B).

Kinking

1. Straight limbs and distinct hinge zones.
2. Internal strain indicates layer-parallel shortening at all levels.
3. Yielding or faulting in tight hinge zones.

These features can be used as rules-of-thumb in order to recognize effects of the idealized processes in monoclines. However, it is clear from the analyses of a few field examples discussed in previous pages that none of the idealized processes adequately accounts for the field observations. In general, we must rely on the general model to interpret the field observations.

The general model accounts remarkably well for the main structural features of the Palisades monocline in the Grand Canyon and the Yampa monocline in Dinosaur National Park; none of the field observations contradicts the theoretical predictions. Further analysis of monoclinal flexuring will require consideration of high amplitudes and relatively complicated, realistic, rheological properties of layers and contacts between layers, and precise definition of structural units.

ACKNOWLEDGMENTS

We especially thank Raymond Fletcher, Stanford University, for advice and assistance with the theory, and David Pollard, U.S. Geological Survey, Menlo Park, California, for criticizing the manuscript. The research reported here was financed by the National Science Foundation Grant No. EAR 76-03273.

APPENDIX 1. DERIVATION OF BASIC EQUATIONS FOR ANALYSIS OF BUCKLING AND DRAPING

This appendix has two purposes. It presents several steps in the derivation of displacements or velocities as well as mean stress for two special cases, *drape folding* and *buckling*, of our general model of monoclinal flexuring. Also, it presents solutions for incompressible and compressible linear elastic or viscous materials. Analogous solutions for power-law elastic or viscous materials and for incompressible, nonlinear elastic materials have been derived in some detail by Johnson (1977, chap. 10). Solutions for linear viscous and power-law viscous materials were first derived by Fletcher (1974, 1977).

The general model of monoclinal flexuring is based on a multilayer with layers of various thicknesses and rheological properties, subjected to both stress and displacement boundary conditions. The solutions we present in the following pages include most aspects of the general model. They do not include second- or higher-order effects, including that of yielding of contacts, treated elsewhere (Honea and Johnson, 1976; Reches and Johnson, 1976), which are required to follow high-amplitude development of monoclinal flexures and to determine conditions required for localization as in kink bands. The solutions do represent a wide range of rheological properties, however, so they are relatively general first-order solutions to the general model of monoclinal flexuring.

One useful feature of the analysis is that the solutions presented here are valid for both drape folding and buckling, as well as for gravity instability. The differences between these modes become apparent only through boundary conditions; the general solutions are identical.

Thus, for drape folding, we specify displacements at the base of the multilayer. For buckling, we specify initial displacements throughout the multilayer as well as layer-parallel shortening. For gravity instability, we specify relative densities of various layers and initial displacements throughout the multilayer. We can, of course, combine all three of these. We do combine the first two in our analyses of buckling. For that model, we assume that the initial displacements throughout the multilayer are produced by differential vertical displacement on a fault or a local fold below. Then we determine the amplification of these displacements as a result of layer-parallel shortening.

Linear Elastic or Viscous Materials

The study of drape folding or buckling of linear elastic or viscous materials is especially simple. We solve the basic differential equations and specify boundary conditions at interfaces between layers. In order for buckling to be possible, the interfaces must be perturbed, but for drape folding they can be flat.

For drape folding, we specify the stress-strain relations for *incompressible* materials in plane strain,

$$s_{xx} = p + 2G(\partial u/\partial x) \tag{4a}$$

$$s_{yy} = p + 2G(\partial v/\partial y) \tag{4b}$$

$$s_{xy} = G(\partial v/\partial x + \partial u/\partial y) \tag{4c}$$

$$s_{zz} = p = (s_{xx} + s_{yy})/2 \tag{4d}$$

or *compressible* materials

$$s_{xx} = (2G + \lambda)(\partial u/\partial x) + \lambda\,(\partial v/\partial y) \quad (5a)$$

$$s_{yy} = (2G + \lambda)(\partial v/\partial y) + \lambda\,(\partial u/\partial x) \quad (5b)$$

$$s_{xy} = G(\partial v/\partial x + \partial u/\partial y) \quad (5c)$$

where s is stress, p is mean stress, u and v are displacements in the x- and y-directions, respectively, G is the shear modulus, and λ is a Lamé constant:

$$\lambda = 2G\nu/(1 - 2\nu). \quad (6)$$

Here ν is Poisson's ratio. For viscous materials, u and v are velocities, and G and λ are coefficients of viscosity (Johnson, 1970, p. 272–276).

Substituting the rheological equations (4) or (5) into the equilibrium equations, we derive, for *incompressible* materials,

$$\partial u/\partial x = -\partial v/\partial y \quad (7a)$$

$$G\,[(\partial^2 u/\partial x^2) + (\partial^2 u/\partial y^2)] + \partial p/\partial x = 0 \quad (7b)$$

$$G\,[(\partial^2 v/\partial x^2) + (\partial^2 v/\partial y^2)] + \partial p/\partial y = -\gamma \quad (7c)$$

Here equation (7a) is the condition of incompressibility and γ is the unit weight of the material (density times acceleration of gravity).

For *compressible materials,*

$$(2G + \lambda)(\partial^2 u/\partial x^2) + (G + \lambda)(\partial^2 v/\partial x\partial y) + G(\partial^2 u/\partial y^2) = 0 \quad (8a)$$

$$(2G + \lambda)(\partial^2 v/\partial y^2) + (G + \lambda)(\partial^2 u/\partial x\partial y) + G(\partial^2 v/\partial x^2) = -\gamma\,. \quad (8b)$$

We solve the equilibrium equations for *incompressible material* by eliminating the mean stress, p, between equations (7b) and (7c) and introducing a displacement function ψ such that

$$u = \partial\psi/\partial y \quad (9a)$$

$$v = -\partial\psi/\partial x \quad (9b)$$

which satisfy the condition of incompressibility, equation (7a). Thus, equations (7) and (9) provide the biharmonic equation in ψ:

$$\partial^4\psi/\partial x^4 + 2(\partial^4\psi/\partial x^2\partial y^2) + \partial^4\psi/\partial y^4 = 0. \quad (10)$$

The sinusoidal solution to equation (10) is

$$\psi = (1/\ell)\{[a + b(\ell y - 1)]\exp(\ell y) - [c + d(\ell y + 1)]\exp(-\ell y)\}\cos(\ell x) \quad (11)$$

where a, b, c, and d are arbitrary constants L is wavelength and ℓ is wave number, $2\pi/L$. Substituting equation (11) into equations (9),

$$u = \partial\psi/\partial y = [(a + b\ell y)\exp(\ell y) + (c + d\ell y)\exp(-\ell y)]\cos(\ell x) \quad (12a)$$

$$v = -\partial\psi/\partial x = \{[a + b(\ell y - 1)]\exp(\ell y) - [c + d(\ell y + 1)]\exp(-\ell y)\}\sin(\ell x). \quad (12b)$$

The mean stress is computed by substituting equations (12a) and (12b) into equations (7) and integrating,

$$p = -2G\ell[b\exp(\ell y) - d\exp(-\ell y)]\sin(\ell x) + p_0 - \gamma y \quad (12c)$$

where p_0 is a constant.

We solve equilibrium equations (8) for *compressible material* by determining displacements,

u and v, that satisfy them. First we eliminate u between the two equations and derive a biharmonic equation in v

$$\partial^4 v/\partial x^4 + 2(\partial^4 v/\partial x^2 \partial y^2) + \partial^4 v/\partial y^4 = 0. \tag{13a}$$

Then we eliminate v between the two equations to derive

$$\partial^4 u/\partial x^4 + 2(\partial^4 u/\partial x^2 \partial y^2) + \partial^4 u/\partial y^4 = 0. \tag{13b}$$

The sinusoidal solution to equation (13a) is

$$v = [(a + b\ell y)\exp(-\ell y) + (c + d\ell y)\exp(\ell y)]\sin(\ell x), \tag{14a}$$

where a, b, c, and d are constants. The differential equation for u, equation (13b), is of the same form as that for v, equation (13a), so the solutions for u and v should be similar. Also, the solutions must satisfy equilibriums equations (8), so we select the cosine solution to equation (13b)

$$u = [(e + f\ell y)\exp(-\ell y) + (g + h\ell y)\exp(\ell y)]\cos(\ell x),$$

where e, f, g, and h are constants. We can eliminate constants $e, \ldots, h$ by expressing them in terms of $a, \ldots, d$. We substitute the equations for the displacements into equations (8) and set the coefficients of terms in $\ell y \exp(-\ell y)$, $\exp(-\ell y)$, $\ell y \exp(\ell y)$ equal to zero. These terms provide four equations with which we can express constants $e, \ldots, h$ in terms of constants $a, \ldots, d$. The result is

$$u = -\{[a + b(\ell y + 4\nu - 3)]\exp(-\ell y) - [c + d(\ell y + 3 - 4\nu)]\exp(\ell y)\}\cos(\ell x). \tag{14b}$$

Here we have ignored effects of the weight of the material; that is, we have set γ in equation (8b) equal to zero. In order for equations (14) to satisfy equation (8b), we must add terms that account for displacements caused by the effects of gravity. We shall not do so.

Thus, we have derived the solution for displacements and mean stress for incompressible material, equations (12), and for compressible material, equations (14). The solutions are also valid for velocities for viscous materials, in which case u and v are velocities instead of displacements, and the material constants are viscosity coefficients instead of elasticity moduli. In order to solve problems where density contrasts and layer-parallel shortening are negligible; that is, in order to solve the *drape-folding* model, we merely specify boundary conditions and determine values for the arbitrary constants, a, b, c, and d. Details of this process are discussed in Appendix 2.

The solution of buckling problems requires a few more concepts which we shall discuss now. In buckling problems we consider the amplification of perturbations of flat surfaces of layers; that is, we determine conditions under which the perturbations grow in amplitude. This is the approach which Fletcher (1974, 1977) has introduced to study folding of viscous materials. According to this approach, we imagine that interfaces between layers are initially nonplanar and that the shapes of the interface surfaces can be expressed in terms of Fourier series. The initial shape, for example, might be a sine form,

$$v_i = \delta_i \sin(\ell x), \tag{15a}$$

where i refers to initial deflection, δ_i is the initial amplitude of the sinusoidal wave, and ℓ is the wave number

$$\ell = 2\pi/L, \tag{15b}$$

where L is wavelength. For viscous materials, v_i remains as the initial displacement of the interface, *not* the initial velocity.

Then, the layers are shortened and thickened uniformly as a result of layer-parallel shortening, producing displacements U and V and, nonuniformly, producing displacements u and v. The uniform stresses are designated S. They are, for *incompressible materials,*

$$S_{xx} = 2G(\partial U/\partial x) + P \tag{16a}$$

$$S_{yy} = 2G(\partial V/\partial y) + P \tag{16b}$$

$$P = (S_{xx} + S_{yy})/2 \tag{16c}$$

and, for *compressible* materials,

$$S_{xx} = (2G + \lambda)(\partial U/\partial x) + \lambda\,(\partial V/\partial y) \tag{17a}$$

$$S_{yy} = (2G + \lambda)(\partial V/\partial y) + \lambda\,(\partial U/\partial x). \tag{17b}$$

The nonuniform stresses are defined in equations (4) and (5). In the linear theory we ignore interactions between uniform and nonuniform states of stress and strain so they can be simply superimposed. Further, for the linear theory, the boundary conditions will be defined for the initial, undeformed boundaries. Thus, the displacements must be infinitesimal for the analysis to be valid.

Boundary Conditions

The boundary conditions are treated the same way for the linear elastic or viscous, incompressible or compressible materials. Figure 13 shows part of a boundary between two elastic materials or between an elastic material and a stress-free surface. The stresses acting on the surface can be expressed in terms of a normal stress, σ_{nn}, and a shear stress, σ_{ns}, which are parallel to local coordinates n and s. The slope angle of the surface is locally θ, the angle between the x-direction and the s-direction (Fig. 13). The stresses acting in the x- and y-directions are σ_{xx}, σ_{yy}, and σ_{xy}, where, according to derivations given earlier, the total stresses are the sums of the uniform and nonuniform stresses,

$$\sigma_{xx} = S_{xx} + s_{xx} \tag{18a}$$

$$\sigma_{yy} = S_{yy} + s_{yy} \tag{18b}$$

$$\sigma_{xy} = s_{xy}. \tag{18c}$$

We can derive the relation between the stresses acting on the surface and the stress components in the x- and y-directions by means of Mohr's circle, and they are

$$\sigma_{nn} = \sigma_{yy}\cos^2\theta + \sigma_{xx}\sin^2\theta - 2\sigma_{xy}\sin\theta\cos\theta \tag{19a}$$

$$\sigma_{ns} = (\sigma_{yy} - \sigma_{xx})\cos\theta\sin\theta + \sigma_{xy}(\cos^2\theta - \sin^2\theta). \tag{19b}$$

Now we introduce an approximation. We assume that the slope angle θ is so small that the sine is approximately equal to the tangent,

$$dv_i/dx = \tan\theta \simeq \sin\theta,$$

and that the cosine is nearly equal to unity. Further, we assume that products of the initial slope and the nonuniform stresses, such as $(s_{xx})(dv_i/dx)$, are negligible, but that products of the initial slope and the uniform stresses are significant. (We already have assumed that products of the uniform stresses and the nonuniform strains and rotations are negligible.) With these assumptions, equations (18) and (19) provide

$$\sigma_{nn} \simeq S_{yy} + s_{yy} = \sigma_{yy} \tag{20a}$$

$$\sigma_{ns} \simeq s_{xy} + (S_{yy} - S_{xx})(dv_i/dx). \tag{20b}$$

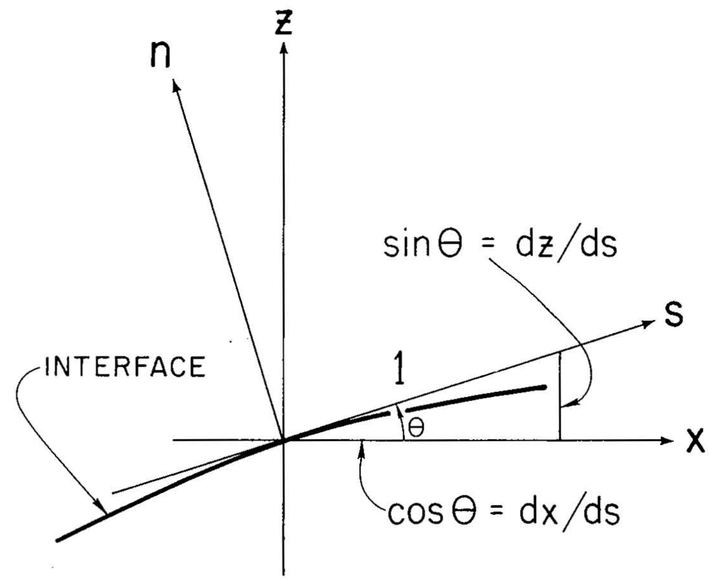

Figure 13. Boundary stresses at the contact between two layers with initial deflection.

One other aspect of boundary conditions must be considered for multilayers with contrast in densities. For such problems we specify that the boundary stresses are satisfied at the initial position of an interface. Thus, if a layer has a thickness of T, then the position of the interface is

$$y = T + v_i,$$

where v_i is the initial deflection of the interface. Then expressions for the mean stress, equations (12c) and (30), include terms such as γv_i, which might "drive" the folding (Ramberg, 1967; Johnson, 1977, p. 371).

Thus, we have presented all the basic equations required to solve problems involving either the drape-folding mode or the buckling mode of our general model of monoclinal flexuring for elastic and viscous materials. We shall discuss some of the details of solutions in Appendix 2.

APPENDIX 2. SOLUTIONS FOR MULTILAYERS

In this appendix we use the general solutions obtained in Appendix 1 to calculate the displacements and strains resulting from drape folding and buckling of a multilayer. We present solutions for incompressible, linear elastic materials, but the solutions are valid for viscous materials in which the displacements are replaced by velocities and the strains by strain rates. First we outline the general method used and then present the solutions for drape folding and for buckling of a multilayer with bonded contacts between layers.

The *sinusoidal solution* for an incompressible elastic material appears in equations (11). The stresses are derived by substituting equations (12) into equations (4),

$$s_{yy} = 2G\ell\{[a + b(\ell y - 1)]\exp(\ell y) + [c + d(\ell y + 1)]\exp(-\ell y)\}\sin(\ell x) - \gamma y + p \quad (21a)$$

$$s_{xx} = -2G\ell\{[a + b(\ell y + 1)]\exp(\ell y) + [c + d(\ell y - 1)]\exp(-\ell y)\}\sin(\ell x) - \gamma y + p \quad (21b)$$

$$s_{xy} = 2G\ell[(a + b\ell y)\exp(\ell y) - (c + d\ell y)\exp(-\ell y)]\cos(\ell x). \quad (21c)$$

Let us rewrite equations (12a) and (12b),

$$u = [(a + b\ell y) \exp(\ell y) + (c + d\ell y) \exp(-\ell y)] \cos(\ell x) \tag{21d}$$

$$v = \{[a + b(\ell y - 1)] \exp(\ell y) - [c + d(\ell y + 1)] \exp(-\ell y)\} \sin(\ell x). \tag{21e}$$

The strains are

$$e_{xx} = \frac{\partial u}{\partial x} = -\ell\,[(a + b\ell y) \exp(\ell y) + (c + d\ell y) \exp(-\ell y)] \sin(\ell x) \tag{21f}$$

$$e_{yy} = -e_{xx} \tag{21g}$$

$$e_{xy} = 1/2\left(\frac{\partial u}{\partial y} + \frac{\partial v}{\partial x}\right) = \ell\,[a + b\ell y) \exp(\ell y) - (c + d\ell y) \exp(-\ell y)] \cos(\ell x). \tag{21h}$$

where e_{xx} and e_{yy} are the normal strains and e_{xy} is the shear strain. Other terms were defined in Appendix 1.

We shall assume that the density of each layer is the same, so that γ is the unit weight of the rock.

Equations (21) are the general solutions for each layer; thus, stresses, displacements, and strains in each layer are determined by four coefficients for each layer, a, b, c, and d. For n layers in the multilayer, there are n sets of equations similar to equations (21), but with different coefficients and shear moduli. One has to solve for all the coefficients to calculate the strains, stresses, and displacements in any layer. This solution, however, is for a single, sinusoidal wavelength, L, whereas a monoclinal flexure may be described in terms of the sum of many wavelengths in the form of a Fourier series. Therefore, we superimpose many (30 or more) wavelengths of the appropriate Fourier series to obtain solutions for monoclinal flexures.

The solutions for drape folding and buckling are essentially identical, only the boundary conditions differ. For drape folding, the initial configuration is a series of flat layers with zero uniform stresses, and the "driving" mechanism for the deformation is the displacement applied at the base. For buckling, the multilayer has an initial monoclinal flexure and is subjected to uniform layer-parallel shortening; the interaction between the uniform stresses and the initial slopes at interfaces of layers is the "driving" mechanism for the growth of the monoclinal flexure.

Drape Folding

In passive folding there are neither uniform stresses nor initial slopes (Fig. 3). Therefore, only the incremental strains and stresses are calculated. For the displacement, V, at the base, we choose the Fourier series (Fig. 14),

$$V = h \sum_{1}^{\infty} a_n \sin \frac{n\pi x}{L}, \tag{22a}$$

where

$$a_n = \frac{2}{n\pi}\left[\cos(n\pi) - \cos\left(\frac{n\pi F}{L}\right)\right] + \frac{1}{\pi}\left[\frac{\sin(\pi/2 + n\pi)}{(N + n)} - \frac{\sin(\pi/2 - n\pi)}{(N - n)}\right] \tag{22b}$$

for $N \neq n$, and

$$a_N = -F/L, \tag{22c}$$

where F is defined in Figure 13, and $N = L/2F$.

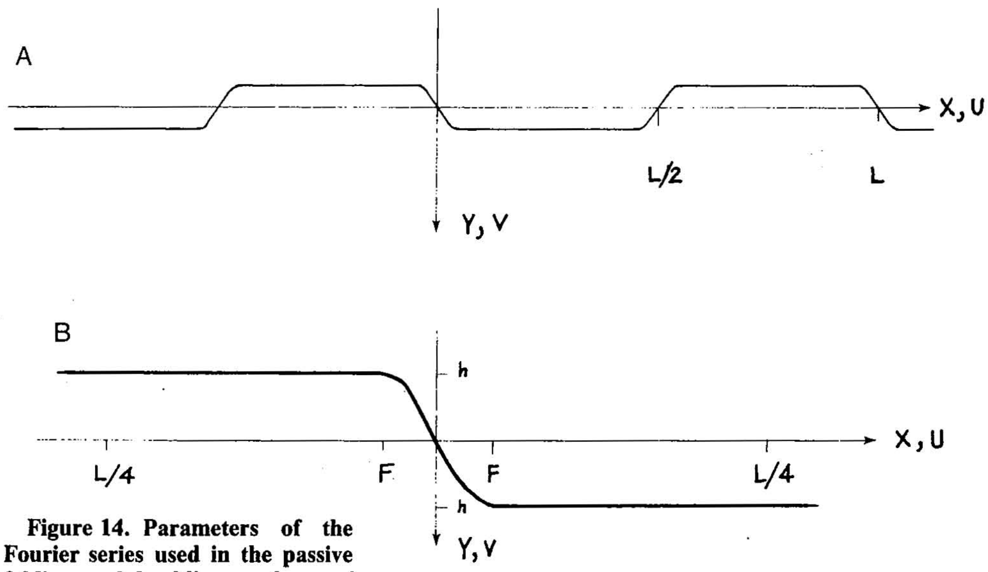

Figure 14. Parameters of the Fourier series used in the passive folding and buckling analyses of monoclinal flexures. (A) The periodic structure assumed. (B) Enlargement of the central part of the structure. $V(x)$ is the monoclinal wave.

$$V(X) = \begin{cases} h & F \leq X \leq L/4 \\ h \sin\left(\frac{\pi X}{2F}\right) & -F \leq X < F \\ -h & -L/4 < X < -F \end{cases}$$

One can vary the width of the flexure at the base from a vertical fault to a wide monoclinal flexure through the factor F (Fig. 14). Our calculations are for the range $F = 0.04\, L_f$ to $F = 0.2\, L_f$, where L_f is the longest wavelength of the Fourier series (Fig. 14).

Equations (21) and (22) should be substituted into the boundary conditions for drape folding. For example, the boundary conditions for the base of the multilayer with bonded contacts are at $y_1 = T_1/2$,

$$(u)_1 = 0 \tag{23a}$$

$$(v)_1 = h\Sigma\,(a)_n \sin\frac{2n\pi x}{L_f}. \tag{23b}$$

Substituting equations (21d), (21e), and (22) into equations (23),

$$a_1 \exp(k_1) + b_1 k_1 \exp(k_1) + c_1 \exp(-k_1) + d_1 k_1 \exp(-k_1) = 0 \tag{24a}$$

$$a_1 \exp(k_1) + b_1 (k_1 - 1) \exp(k_1) - c_1 \exp(-k_1) - d_1 (k_1 + 1) = h(a)_n, \tag{24b}$$

where $k_1 = T_1\ell/2$, $\ell = 2\pi n/L_f$, and $(a)_n$ is the coefficient of the Fourier series.

Similarly, by substituting equations (31) into the boundary conditions for drape folding of a bonded multilayer (Reches, 1977), a system of $4n$ linear equations is derived,

$$[\mathbf{A}] \cdot [\mathbf{X}] = [\mathbf{B}], \tag{25}$$

where **A** is the matrix of known constants, **X** is the vector of the unknown coefficients $a_1, b_1, c_1, d_1, a_2, \ldots, c_n, d_n$ and **B** is the vector of the "driving" terms (Reches, 1977). The "driving" terms are the displacements at the base in passive folding. The system of linear equations is solved by regular subroutines for simultaneous solutions which are available in any computation center.

After solving equations (24) for a single wavelength, we substitute the vector **X** of coefficients into equations (21) and calculate the strains and displacements within each layer. We repeat this procedure for at least thirty wavelengths defined by the Fourier series, equation (22).

Thereafter, we sum the strains and displacements to give the final results, which are summarized in several diagrams (Figs. 6, 7).

The procedure for drape folding of multilayer with frictionless contacts is essentially the same, but with different boundary conditions (Reches, 1977).

Buckling

We consider the buckling of a multilayer with initial monoclinal deflection over an infinite medium (Figs. 8, 9). Both the multilayer and the medium are subjected to horizontal shortening, $\partial U / \partial x$. Using equations (7a), (4a) (4b), and (15a), we rewrite equations (19),

$$\sigma_{nn} = S_{yy} + s_{yy} \tag{26a}$$

$$\sigma_{ns} = s_{xy} - 4G(\partial U / \partial x)\, dv_i / dx, \tag{26b}$$

where σ_{nn} is the normal stress and σ_{ns} is the shear stress at a contact, and dv_i / dx is the initial slope. The initial slope dv_i / dx is calculated for every layer by means of the drape-folding analysis described in earlier paragraphs and then substituted into the boundary conditions for buckling, equations (26).

Let us derive the boundary conditions for one contact as an example. We choose the contact between the lower medium and the multilayer, assuming bonded contacts. The coefficients, a_m and b_m, for the medium must vanish to satisfy the conditions of vanishing stresses and displacements for y_m approaching infinity, because these coefficients are associated with positive exponents, equations (21). Therefore, at the contact

$$y_m = \delta_i \sin (\ell x);\ y_1 = T_1 / 2 + \delta_i \sin (\ell x),$$

the boundary conditions are (Table 5)

$$(\sigma_{nn})_m - (\sigma_{nn})_1 = 0 \tag{27a}$$

$$(\sigma_{ns})_m - (\sigma_{ns})_1 = 0 \tag{27b}$$

$$(u)_m - (u)_1 = 0 \tag{27c}$$

$$(v)_m - (v)_1 = 0 \tag{27d}$$

Substituting equations (21) and (26) into equations (27) yields the following equations:

$$\begin{aligned} -c_m R_m + d_m R_m + a_1 \exp (k_1) + b_1 (k_1 - 1) \exp (k_1) + c_1 \exp (-k_1) \\ + d_1 (k_1 + 1) \exp (-k_1) = 0 \end{aligned} \tag{28a}$$

$$\begin{aligned} c_m R_m + 0 + a_1 \exp (k_1) + b_1 k_1 \exp (k_1) - c_1 \exp (-k_1) \\ + d_1 \exp (-k_1) = 4(\partial U / \partial x)(1 - R_m) \partial V / \partial x) \end{aligned} \tag{28b}$$

$$-c_m + 0 + a_1 \exp (k_1) + b_1 k_1 \exp (k_1) + c_1 \exp (-k_1) + d_1 \exp (-k_1) = 0 \tag{28c}$$

$$\begin{aligned} c_m + d_m + a_1 \exp (k_1) + b_1 (k_1 - 1) \exp (k_1) - c_1 \exp (-k_1) \\ - d_1 (k_1 + 1) \exp (-k_1) = 0 \end{aligned} \tag{28d}$$

where $k_1 = T_1 \ell / 2$, $\ell = 2\pi n / L_f$, and $R_m = G_m / G_i$.

Similarly, by substituting equations (21) and (26) into the boundary conditions, we obtain a system of $4n$ linear equations for the bonded multilayer (Reches, 1977),

$$[\mathbf{A}] \cdot [\mathbf{X}] = [\mathbf{B}] \tag{29}$$

where **A** is the matrix of the known constants, **X** is the vector of the unknown coefficients c_m, d_m, a_1, b_1, . . . , c_n, d_n, and **B** is the vector of "driving" terms (Reches, 1977).

The "driving" terms in the buckling case are the products of the initial slopes, the uniform strain and a shear modulus, equations (26b) and (28b). The system of linear equations is solved by regular subroutines for simultaneous equations. In a manner similar to the calculations of drape folding, we repeat the computations for at least thirty wavelengths of the Fourier series, and we sum the displacements and strains (Figs. 8, 9). The procedure for analysis of buckling of a multilayer with frictionless contacts is essentially the same, but with different boundary conditions (Reches, 1977).

A term involving the unit weight of the rock would enter the equation for the normal stress at the free upper surface, but for convenience it has been deleted in our analysis. Specific consideration of its effect would require that another variable be specified. Its effect, however, is clearly that of reducing amplitudes of folding near the free surface, the amount depending upon the relative magnitudes of the uniform horizontal stress, S_{xx}, and the product, $\delta_i\gamma$.

REFERENCES CITED

Baker, A. A., 1935, Geological structure of southeastern Utah: Am. Assoc. Petroleum Geologists Bull., v. 19, p. 1472–1507.

Biot, M. A. Ode, H., and Roever, W. L., 1961, Experimental verification of the folding of stratified viscoelastic media: Geol. Soc. America Bull., v. 72, p. 1621–1630.

Chapple, W. M., and Spang, J. H., 1974, Significance of layer-parallel slip during folding of layered sedimentary rocks: Geol. Soc. America Bull., v. 85, p. 1523–1534.

Clark, S. P., Jr. (ed.), 1966, Handbook of physical constants: Geol. Soc. America Mem. 97, 587 p.

Cook, R. A., 1975, Mechanisms of sandstone deformation: A study of the drape-folded Weber sandstone in Dinosaur National Monument, Colorado and Utah [Ph.D. dissert.]: College Station, Texas A & M Univ.

Cook, R. A., and Stearns, D. W., 1975, Mechanisms of sandstone deformation: A study of the drape-folded Weber Sandstone in Dinosaur National Monument, Colorado and Utah: Rocky Mtn. Assoc. Geol., 1975 Symposium, p. 21–32.

Dietrich, J. H., and Carter, N. L., 1969, Stress-history of folding: Am. Jour. Sci., v. 267, p. 129–154.

Dutton, C. E., 1882, Tertiary history of the Grand Canyon District: U.S. Geol. Survey Mon. 2, 264 p.

Fletcher, R. C., 1974, Wavelength selection in the folding of a single layer with power-law rheology: Am. Jour. Sci., v. 274, p. 1029–1043.

—— 1977, Folding of a single viscous layer: Exact infinitesimal-amplitude solution: Tectonophysics, v. 39, p. 593–606.

Fletcher, R. C. and Sherwin, Jo-Ann, 1978, Relation between observed fold arc length and theoretical preferred wavelength in single-layer folding: Am. Jour. Sci. (in press).

Friedman, M., Handin, J., Logan, J. M., Min, K. D., and Stearns, D. W., 1976, Experimental folding of rocks under confining pressure: Pt. III. Faulted drape folds in multilithologic layered specimens: Geol. Soc. America Bull., v. 87, p. 1049–1066.

Honea, E., and Johnson, A. M., 1976, A theory of concentric, kink, and sinusoidal folding and of monoclinal flexuring of compressible, elastic multilayers. Pt. IV, Development of sinusoidal and kink folds in multilayers confined by rigid boundaries: Tectonophysics, v. 30, p. 197–239.

Howard, J. H., 1966, Structural development of the Williams Range thrust, Colorado: Geol. Soc. America Bull., v. 77, p. 1247–1264.

Hudleston, P. J., 1973, An analysis of "single-layer" folds developed experimentally in viscous media: Tectonophysics, v. 16, p. 189–214.

Hudleston, P. J., and Stephansson, O., 1973, Layer shortening and foldshape development in buckling of single layers: Tectonophysics, v. 17, p. 299–321.

Johnson, A. M., 1970, Physical processes in geology: San Francisco, Freeman, Cooper and Co., 577 p.

—— 1977, Styles of folding: New York, Elsevier Pub. Co., 406 p.

Johnson, A. M., and Ellen, S. D., 1974, A theory of concentric, kink, and sinusoidal folding and of monoclinal flexuring of compressible, elastic multilayers. Pt. I, Introduction: Tectonophysics, v. 21, p. 301–339.
Johnson, A. M., and Page, B. M., 1976, A theory of concentric, kink, and sinusoidal folding and of monoclinal flexuring of compressible, elastic multilayers. Pt. VII, Development of folds within Huasna syncline, San Luis Obispo County, California: Tectonophysics, v. 33, p. 97–143.
Johnson, A. M., and Pollard, D. D., 1971, Mechanics of intrusion of laccoliths: Final rept. to NSF, Branner Library, Stanford Univ., Calif. 173 p.
Kelley, V. C., 1955, Monoclines of the Colorado Plateau: Geol. Soc. America Bull., v. 66, p. 789–804.
Logan, J. M., Friedman, M., and Stearns, M. T., 1978, Experimental folding of rocks under confining pressure: Pt. VI. Further studies of faulted drape-folds, *in* Matthews, V., ed., Folding associated with the basement faulting in the Rocky Mountain region: Geol. Soc. America Mem. 151 (this volume).
Min, K. D., 1974, Analytical and petrofabric studies of experimental faulted drape folds in layered rock specimens Ph.D. dissert.: College Station, Texas A & M Univ., 90 p.
Powell, J. W., 1873, Exploration of the Colorado River of the West and its tributaries explored in 1869–1872: Washington D.C., Smithsonian Inst., 291 p.
Prucha, J. J., Graham, J. A., and Nickelsen, R. P., 1965, Basement-controlled deformation in Wyoming province of Rocky Mountains foreland: Am. Assoc. Petroleum Geologists Bull., v. 49, p. 966–992.
Ramberg, H., 1967, Gravity, deformation, and the earth's crust: New York, Academic Press, 214 p.
——1970, Folding of laterally compressed multilayers in the field of gravity: Physics Earth and Planetary Interiors, p. 203–232.
Ramberg, I. B., and Johnson, A. M., 1976, Asymmetric folding in interbedded chert and shale of the Franciscan Complex, San Francisco Bay area, California: Tectonophysics, v. 32, p. 295–320.
Ramberg, H., and Strömgård, K. E., 1971, Experimental tests of modern buckling theory applied on multilayered media: Tectonophysics, v. 11, p. 461–472.
Reches, Z., 1977, The development of monoclines [Ph.D. dissert.]: Dept. Geology, Stanford Univ., 234 p.
——1978, Structure of the Palisades Creek branch of the East Kaibab monocline, Grand Canyon, Arizona: *in* Matthews, V., ed., Folding associated with the basement faulting in the Rocky Mountain region: Geol. Soc. America Mem. 151 (this volume).
Reches, Z., and Johnson, A. M., 1976, A theory of concentric, kink, and sinusoidal folding and of monoclinal flexuring of compressible, elastic multilayers. Pt. VI, Asymmetric folding and monoclinal kinking: Tectonophysics, v. 35, p. 295–335.
Sanford, A. R., 1959, Analytical and experimental study of simple geologic structures: Geol. Soc. America Bull., v. 70, p. 19–52.
Sherwin, J. A., and Chapple, W. M., 1968, Wavelengths of single-layer folds: A comparison between theory and observation: Am. Jour. Sci., v. 266, p. 167–179.
Stearns, D. W., 1971, Mechanisms of drape folding in the Wyoming province: Wyoming Geol. Assoc., 23rd Ann. Field Conf. Guidebook, p. 125–143.
Treagus, S. H., 1973, Buckling stability of a viscous single-layer system, oblique to the principal compression: Tectonophysics, v. 19, p. 271–289.
Walcott, C. D., 1890, Study of line of displacement in the Grand Canyon of the Colorado in northern Arizona: Geol. Soc. America Bull., v. 1, p. 49–64.
Willis, B., 1894. Mechanics of Appalachian structure: 13th Ann. Rept. of the U.S. Geol. Survey, 1891–92, p. 213–281.
Zanemonets, V. B., Mikhaylov, V. O., and Myasnikov, V. P., 1976, A mechanical model of the deformation of block folding: Izvestia Physics of the Solid Earth, no. 10, p. 13–21.

MANUSCRIPT RECEIVED BY THE SOCIETY JUNE 27, 1977
MANUSCRIPT ACCEPTED AUGUST 25, 1977